HHS Public Access

Author manuscript

Arch Biochem Biophys. Author manuscript; available in PMC 2018 October 15.

Published in final edited form as:

Arch Biochem Biophys. 2017 October 15; 632: 142–157. doi:10.1016/j.abb.2017.07.005.

Structure, function, and mechanism of proline utilization A (PutA)

Li-Kai Liu[a], **Donald F. Becker**[b,*], and **John J. Tanner**[a,c,*]

[a]Department of Biochemistry, University of Missouri, Columbia, MO, United States

[b]Department of Biochemistry and Redox Biology Center, University of Nebraska-Lincoln, Lincoln, NE, 68588-0664, United States

[c]Department of Chemistry, University of Missouri, Columbia, MO, United States

Abstract

Proline has important roles in multiple biological processes such as cellular bioenergetics, cell growth, oxidative and osmotic stress response, protein folding and stability, and redox signaling. The proline catabolic pathway, which forms glutamate, enables organisms to utilize proline as a carbon, nitrogen, and energy source. FAD-dependent proline dehydrogenase (PRODH) and NAD^+-dependent glutamate semialdehyde dehydrogenase (GSALDH) convert proline to glutamate in two sequential oxidative steps. Depletion of PRODH and GSALDH in humans leads to hyperprolinemia, which is associated with mental disorders such as schizophrenia. Also, some pathogens require proline catabolism for virulence. A unique aspect of proline catabolism is the multifunctional proline utilization A (PutA) enzyme found in Gram-negative bacteria. PutA is a large (> 1000 residues) bifunctional enzyme that combines PRODH and GSALDH activities into one polypeptide chain. In addition, some PutAs function as a DNA-binding transcriptional repressor of proline utilization genes. This review describes several attributes of PutA that make it a remarkable flavoenzyme: (1) diversity of oligomeric state and quaternary structure; (2) substrate channeling and enzyme hysteresis; (3) DNA-binding activity and transcriptional repressor function; and (4) flavin redox dependent changes in subcellular location and function in response to proline (functional switching).

Keywords

flavoprotein; flavin-dependent reaction; protein structure; proline catabolism; multifunctional enzymes; substrate channeling; aldehyde dehydrogenase; enzyme hysteresis

[*]**Corresponding authors**. Donald F. Becker, Department of Biochemistry and Redox Biology Center, University of Nebraska, Lincoln, NE, 68588-0664, dbecker3@unl.edu; and John J. Tanner, Department of Biochemistry, University of Missouri, Columbia, MO 65211; tannerjj@missouri.edu.

Introduction

Proline is catabolized to glutamate in two enzymatic steps (Fig. 1A). The flavoenzyme proline dehydrogenase (PRODH) catalyzes the 2-electron oxidation of proline with the concomitant reduction of a flavin cofactor, which is typically FAD (reductive-half reaction). This reaction is coupled to the reduction of the second substrate found in the membrane (e.g., ubiquinone), which in turn re-oxidizes the reduced flavin, enabling another round of catalysis (oxidative-half reaction). The product of the PRODH reaction, Δ^1-pyrroline-5-carboxylate (P5C), undergoes non-enzymatic hydrolysis to acyclic L-glutamate-γ-semialdehyde, (GSAL). Finally, GSAL is converted to glutamate by GSAL dehydrogenase (GSALDH) via an NAD^+-dependent 2-electron oxidation reaction.

Inborn deficits in PRODH and GSALDH in humans lead to hyperprolinemia I [1, 2] and II [3, 4], respectively. Deficiencies in PRODH are associated with schizophrenia and related neurological disorders [1, 5–7]. In this regard, elevated proline levels in *Prodh*$^{-/-}$ mice were found to inhibit glutamate decarboxylase, resulting in lower production of γ-aminobutyric acid (GABA) and lower GABA-ergic transmissions [8]. PRODH also has an important role in the metabolic changes associated with cancer [9–12]. Recently, down-regulation of PRODH, either by small molecule inhibition or knockdown, was shown to significantly reduce breast tumor cell growth in spheroid cultures and metastasis in mouse models of breast cancer [12]. PRODH activity helps drive ATP synthesis due to coupling of proline oxidation with reduction of ubiquinone in the mitochondrial electron transport chain [12–14]. Proline catabolism also drives production of reactive oxygen species, which has been shown to induce apoptosis in mammal cells [9, 15, 16] and prolong life span of *Caenorhabditis elegans* [17]. The formation of hydrogen peroxide as a by-product of proline oxidative catabolism appears to be a feature of proline metabolism that is conserved in bacteria, plants, and animals [18–20].

Curiously, in certain Gram-negative bacteria, the PRODH and GSALDH activities are combined into a single polypeptide, known as proline utilization A (PutA) [21]. PutAs enable bacteria to utilize proline as a source of carbon and nitrogen when grown under poor nutrient conditions [21]. The utilization of proline by PutA contributes to the pathophysiology of Gram-negative pathogens such as *Helicobacter pylori* [22, 23] and *Ehrlichia chaffeensis* [24]. These pathogens invade host microenvironments that are abundant in proline. *H. pylori* resides in the upper gastrointestinal tract where proline levels have been estimated to be 10-fold higher in infected patients relative to control patients [25]. Additionally, PutAs are excellent systems for fundamental studies of substrate channeling and redox-linked allosteric activation of protein function (aka, functional switching) [26–28]. Herein we review the structures, functions, and molecular mechanisms of PutAs, emphasizing the attributes that make PutA unique among flavin-dependent dehydrogenases.

Classification of PutAs

PutAs are classified according to a combination of domain architecture (Fig. 1B) and sequence similarity (Fig. 1C) [29]. Three domain architectures are known (types A, B, and C). Architecture type A PutAs are about 1000 residues long and have a minimal domain set

consisting of N-terminal PRODH and C-terminal GSALDH modules. The type B PutAs have an additional 100–200 residue C-terminal domain, which was recently shown to be a structural domain having the aldehyde dehydrogenase superfamily (ALDHSF) fold [29, 30]. Type C PutAs contain both the C-terminal ALDHSF domain and an N-terminal ribbon-helix-helix (RHH) DNA-binding domain, the latter endowing these PutAs with transcriptional repressor functionality. Alignment of PutA protein sequences yield a phylogenetic tree with three main branches (branch 1, 2 or 3) (Fig. 1C). Combining the domain architecture information with sequence similarity yields a unified classification scheme consisting of five PutA classes designated by the branch number of the tree followed by the domain architecture type: 1A, 1B, 1C, 2A, and 3B [29] (Table 1).

Three-dimensional structure of PutA

The fold and oligomeric states of type A PutA

Type A PutAs were the first family members to be characterized by high-resolution crystallography (Table 2). The structure of the class 1A PutA from *Bradyrhizobium japonicum* (BjPutA, 999 residues) was reported in 2010 [31]. A few years later, several structures of the 2A PutA from *Geobacter sulfurreducens* (GsPutA, 1004 residues) appeared [32]. The GsPutA catalog includes complexes of the oxidized enzyme with proline analogs, structures of the enzyme in the 2-electron FAD reduced state, and a structure with the model electron acceptor menadione bisulfite (MB) bound in the PRODH active site. Also, the structure of another class 2A PutA was reported recently (PutA from *Bdellovibrio bacteriovorus*, BbPutA) [33].

Type A enzymes have the same basic fold consisting of seven domains – arm, α domain, PRODH $(\beta\alpha)_8$-barrel catalytic domain, linker, Rossmann NAD^+-binding domain, GSALDH catalytic domain, and oligomerization domain (Fig. 2A). Despite the low global sequence identity (27%), BjPutA and GsPutA exhibit high overall structural similarity, with a root mean square deviation of 2.0 Å for 800 residues. The root mean square deviation between the class 2A PutA structures (GsPutA and BbPutA) is only 1.1 Å, as expected for two proteins with high sequence identity (47%). The PRODH active site is located in a $(\beta\alpha)_8$ barrel, which binds FAD. The GSALDH module features a Rossmann dinucleotide-binding domain and an α/β catalytic domain bearing a conserved nucleophilic cysteine. The GSALDH module is typical for ALDHSF enzymes. The oligomerization domain also is typical of ALDHSF enzymes and mediates the classic ALDHSF mode of domain-swapped dimerization in type A PutA (described below).

The structural basis for substrate channeling is evident in the protein fold. The two active sites are separated by a linear distance of 45 Å and connected by a curved tunnel that traverses 65 Å and ranges in radius from 1.5 Å near the active sites to 4.5 Å in the middle section (Fig. 2A). The tunnel is predominantly hydrophilic, which is consistent with P5C/GSA having polar and charged functional groups. Presumably the tunnel of the resting enzyme contains water molecules. Some of these are observed as ordered water molecules in electron density maps. However, the tunnel also has substantial space that has been left unmodeled in the PutA structures, suggesting the tunnel contains mobile water molecules that emulate bulk water. Several conserved residues appear on both ends of the tunnel near

the two active sites. In particular, a Glu-Arg ion pair (Glu149-Arg421 in GsPutA) is universal to all PutA PRODH domains (and monofunctional PRODHs [34]), and its gating activity is thought to be critical to control proline substrate binding and P5C release [32].

The tunnel of BjPutA was explored with tunnel-blocking mutagenesis, in which bulky side chains are installed at various positions lining the tunnel [35]. These studies showed that even small reductions in the tunnel radius impede channeling, suggesting the width of the tunnel closely matches the size of the channeled intermediate. An implication is that there is not enough room for the intermediate to rotate during transit from the PRODH to the GSALDH active site. This suggests the intermediate likely enters the tunnel at the PRODH end with a specific orientation that facilitates proper substrate binding at the GSALDH end.

Type A PutAs form domain swapped-dimers mediated by an oligomerization domain (Fig. 3). This type of dimer is characteristic of the ALDHSF. The oligomerization domain is a bipartite flap-like substructure consisting of a β-hairpin protruding from the GSALDH Rossmann NAD^+-binding domain and the C-terminal ~25 residues of the polypeptide chain (Fig. 2A). In the dimer, the oligomerization domain of one protomer forms an intermolecular β-sheet interaction with the GSALDH catalytic domain of the opposite protomer.

Domain-swapped dimerization in type A PutA plays a very important functional role. The β-flap of the oligomerization domain of one protomer covers the wide middle section of the substrate-channeling tunnel of the opposite protomer. Without this lid, the intermediate would have a higher probability of dissociating from the enzyme. Thus, dimerization enables substrate-channeling in type A PutAs. This is a good example of how quaternary structure contributes directly to a step in the kinetic mechanism of an enzyme.

Interestingly, in BjPutA, two of the domains-swapped dimers assemble into a ring-shaped tetramer (Fig. 3). No other PutA studied to date forms this tetramer, so its functional significance is a matter of speculation. Recently, Korasick and coworkers showed that engineered dimeric forms of BjPutA retain full catalytic activity, suggesting that tetramerization is not essential for *in vitro* activity [33]. Whether the tetramer is needed for *in vivo* function remains to be studied.

The structures of type B PutA reveal the fold and functions C-terminal ALDHSF domain

Structures of type B PutAs from *Sinorhizobium meliloti* (SmPutA) [30] and *Corynebacterium freiburgense* (CfPutA) [29] confirmed the conservation of the PutA fold and revealed the structure and functions of the C-terminal ALDHSF domain. Type B PutAs have 6 of the 7 domains seen in type A PutAs, plus the C-terminal domain, which is not found in type A PutAs (Fig. 2B). Type B PutAs lack the oligomerization domain of type A PutA, which results in a different mode of oligomerization (described below). The similarity between type A and type B PutAs can be quantified using the using the secondary-structure matching (SSM) algorithm via the PDBeFold server [36]. The rmsd between the type A structures and SmPutA is 1.7 Å covering 980 residues. This suggests that SmPutA contains the majority of the type A PutA fold within it. In fact, ~77% of the secondary structural elements in type A PutA are also in SmPutA. The type A structures are less similar to class 3B PutA CfPutA, with rmsd of 2.1 – 2.7 Å covering ~700 residues. A peculiarity of the

CfPutA structure is that the α-domain and part of the PRODH domain that binds proline are disordered in the crystal. As a result, the PRODH active site exhibits an atypically open conformation in which the isoalloxazine is more exposed than in other PutA structures. Because of these unusual features, the CfPutA structure may represent an inactive form of the enzyme that exists prior to hysteretic activation [29]. Hysteresis in PutA is described below. Nevertheless, CfPutA contains 69% of the secondary structural elements found in type A PutA structures. In summary, the type A PutA fold is conserved in type B PutAs, except for the oligomerization domain, which is absent in type B PutA.

The structural similarity between type A and type B PutA also extends to the substrate-channeling tunnel. In type B PutA, the two actives sites are separated by approximately 40 Å and connected by a tunnel that has the same dimensions as in type A PutAs. Thus, the structures imply a conserved mechanism of substrate channeling.

Type B PutA contains an additional C-terminal domain not found in type A PutA (Fig. 1B). The C-terminal domain spans about 200 residues and consists of an α/β sub-domain fused to a β-flap [29, 30]. Curiously, the α/β sub-domain resembles the Rossmann fold found in all ALDHs, including the GSALDH module of PutA. Furthermore, the β-flap of the C-terminal domain resembles the oligomerization flap found in other ALDHs, including type A PutA. Because of these similarities, the C-terminal domain is referred to as the “C-terminal ALDHSF domain”. See Luo et al. for a detailed discussion of the striking structural homology between the PutA C-terminal domain and ALDHSF enzymes [30].

Because of structural homology between the C-terminal domain and ALDHSF enzymes, type B PutAs have two Rossmann fold domains, one in the GSALDH module (Rossmann 1) and another in the C-terminal domain (Rossmann 2). This is unexpected, since the reaction catalyzed uses only one NAD^+ per round of catalysis. Structural studies have shown that the C-terminal ALDHSF domain does not bind NAD^+ [29, 30]. As discussed by Luo et al. [30], the surface where one would expect NAD^+ to dock to the C-terminal domain is unlike a *bona fide* Rossmann NAD^+-binding domain. In particular, the narrow groove expected for the adenine has been converted to a wide, flat valley, and side chains and loops invade the space where the nicotinamide riboside and adenine ribose groups would bind. These variations prevent NAD^+ from binding to the C-terminal ALDHSF domain.

The C-terminal ALDHSF domain contains a β-flap substructure. It is a bipartite element consisting of a β-hairpin protruding from the Rossmann sub-domain and ~25 residues of the C-terminal polypeptide chain (Fig. 2B). The flap strongly resembles the classic ALDHSF oligomerization flap. However, the flap does not mediate oligomerization in type B PutA. Rather, the β-flap of the C-terminal domain interacts intramolecularly with the sheet of the GSALDH catalytic domain, effectively extending the β-sheet to help stabilize the aldehyde substrate binding site. Furthermore, the β-flap of the C-terminal domain forms a cap over the substrate-channeling tunnel that mimics the quaternary structural interactions found in the type A PutA domain-swapped dimer. Therefore, the tertiary structural interactions formed by the C-terminal domain within the type B PutA monomer mimic the quaternary structural interactions in the type A dimer (Fig. 3).

Recently, Korasick and coworkers used domain-deletion analysis to probe the function of the C-terminal ALDHSF domain in CfPutA [29]. Deletion of the C-terminal ALDHSF domain abrogates GSALDH activity, which supports the hypothesis proposed by Luo et al. [30, 37] that the β-flap of the C-terminal domain stabilizes the aldehyde binding site. Somewhat surprisingly, deletion of the C-terminal ALDHSF domain also greatly diminished the PRODH activity of CfPutA [29]. This result can be rationalized by noticing that the β-flap of the C-terminal domain makes extensive contacts with the PRODH barrel. Apparently, these contacts are necessary for stabilizing the active conformation of the PRODH active site.

The novel dimerization of type B PutA

Because of the C-terminal ALDHSF domain, type B PutAs have different quaternary structures compared to type A PutAs. SAXS studies of the type B PutA from *Rhodobacter capsulatus* (RcPutA) indicated a monomeric protein in solution [37]. SAXS analysis of SmPutA showed the enzyme forms a concentration-dependent monomer-dimer equilibrium [30]. Combining the SAXS data and crystal structures allowed elucidation of the dimer structure. The C-terminal ALDHSF domain features prominently in the dimer interface of 1800 $Å^2$, where the C-terminal ALDHSF domain of one protomer packs against several α-helices of the catalytic modules. Notably, the β-flap of the C-terminal domain is not involved in dimerization, which is paradoxical given the structural similarity of the flap to the oligomerization domain of type A PutA.

Studies of CfPutA have revealed a more complex mechanism of self-association behavior whereby ligand binding to the active site enhances oligomerization [29]. Initial sedimentation velocity experiments performed in the absence of active site ligands suggested a strictly monomeric protein, even at the high concentration of 6 mg/ml (50 μM). We note that SmPutA is ~50% dimeric at this concentration. However, in the presence of the proline analog L-tetrahydro-2-furoic acid (THFA) and NAD^+, a higher molecular mass species appeared in the distribution curves from sedimentation velocity. The second species corresponds to a dimer, and its concentration increases with increasing protein concentration. These results suggest the oligomeric state of CfPutA in solution is influenced by both the occupancy of the proline substrate site and protein concentration. The preliminary interpretation of these results is that type B PutA may adhere to the morpheein model of enzyme hysteresis [38, 39], in which substrate binding induces conformational changes that promote assembly of a high-activity oligomer. Additional research is needed to determine whether this phenomenon is idiosyncratic to CfPutA or conserved by PutAs that contain the C-terminal ALDHSF domain. Furthermore, studies are needed to determine whether ligand-linked oligomerization regulates the catalytic activity of PutA, as expected for a morpheein-type enzyme.

The structure of type C PutA

Although a crystal structure of type C PutA is not available, much is known about the structure at low resolution from small-angle X-ray scattering (SAXS), biochemical studies, and analogy with type B PutA (Fig. 4). Much of this work has been done on the archetypal 1C PutA from *Escherichia coli* (EcPutA, 1320 residues). Amino acid sequence alignment of

EcPutA and the 1B SmPutA indicates 60% identity over ~1200 residues. The region of sequence similarity spans the entire SmPutA sequence and includes all but residues ~1–85 of EcPutA. This result suggests that the SmPutA structure is a good model for the catalytic part of EcPutA. Also, the crystal structure of the isolated ribbon-helix-helix (RHH) domain has been determined [40, 41]. Thus, the main challenges of type C structural biology are to determine the structure of the RHH-arm linker, the tertiary structural interactions formed by the RHH and RHH-arm linker, and the quaternary structure. We next summarize the current models of EcPutA.

Type C PutAs have a quaternary structure not seen in other PutAs, which reflects its unique transcriptional repressor function. SAXS showed that EcPutA forms an elongated V-shaped dimer with radius of gyration (R_g) of 63 Å and dimensions of 205 × 85 × 55 Å [42]. Domain deletion analysis and SAXS rigid body modeling show the RHH domain mediates dimerization at the centroid of the particle, and the catalytic modules (residues 85–1320) reside in the large outer lobes. Obviously, the lack of an RHH domain precludes this mode of dimerization in types A and B PutAs.

We note the structure of the C-terminal domain and its tertiary structural interactions with other PutA domains were not known at the time we made the EcPutA SAXS model [42]. Here we present a more complete model with the DNA-binding domain dimer (PDB 2GPE) and residues 87–1320 built by combining the crystal structure of an EcPutA PRODH domain construct (PutA86-630, PDB code 4O8A [43]) with a homology model based on the SmPutA structure (PDB code 5KF6) generated with SWISS-MODEL [44] (Fig. 4).

The catalytic mechanism of the PRODH module of PutA

The PRODH module of PutA contains an FAD cofactor that couples the oxidation of proline (reductive half-reaction) to the reduction of ubiquinone in the membrane (oxidative half-reaction) [45]. The reductive half-reaction involves proline binding, flavin reduction, isomerization, and product dissociation [46]. The oxidative mechanism includes the binding of ubiquinone to reduced PutA, oxidation of the reduced flavin, and an isomerization step to regenerate the native conformation [46].

Early kinetic analysis of the class 1C PutA from *Salmonella typhimurium* suggested a ping-pong mechanism for the PRODH activity [47]. A ping-pong mechanism for the PRODH activity of the class 1C EcPutA was also demonstrated with dead-end inhibition using L-proline and ubiquinone analogs [45]. The steady-state kinetic assays including product inhibition with P5C show that EcPutA PRODH follows a two-site ping-pong mechanism, similar to that observed with other flavin-dependent oxidoreductases [45]. Later, stopped-flow kinetic measurements supported the mechanism by examining the microscopic steps in the reductive and oxidative half-reactions [46]. The rate-limiting step was found to be in the oxidative half-reaction involving oxidation of the flavin by quinone [46]. Moreover, isomerization steps were observed in both half-reactions and were proposed to represent different conformers generated by changes in the redox state of the flavin [46]. The isomerization steps are proposed to be required for functional switching of EcPutA (discussed in “Functional switching” below) [46, 48].

The catalytic mechanism of the GSALDH module of PutA

The fold and catalytic mechanism of the GSALDH module are representative of ALDHSF enzymes. In both PutAs and monofunctional GSALDHs, NAD^+ binds to the Rossmann fold domain in an extended conformation that positions the nicotinamide near the catalytic Cys residue of the GSALDH catalytic domain [3, 30, 31, 49]. This is the canonical binding mode for Rossmann fold enzymes [50, 51]. Structures of GSALDHs complexed with the product glutamate imply that GSAL binds with its α-carboxylate and amino group interacting with a conserved loop known as the "anchor loop". The importance of the anchor loop has been investigated in monofunctional GSALDH [3, 49]. The carbonyl O atom of the aldehyde group of GSAL binds in the oxyanion hole, which consists of two hydrogen bond donors - a conserved Asn side chain and the backbone of the catalytic Cys. The catalytic Cys residue, anchor loop, and oxyanion hole Asn residue are present in all PutAs and GSALDHs.

The accepted mechanism of ALDHs begins with nucleophilic attack by the catalytic Cys on the aldehyde of the substrate, producing a tetrahedral hemithioacetal intermediate (Fig. 5A). In this step, the aforementioned oxyanion hole stabilizes the negatively charged O atom of the intermediate. Hydride transfer to NAD^+ generates NADH and the acyl-enzyme intermediate. Next, a conserved Glu residue activates the water molecule that attacks the acyl-enzyme intermediate. This Glu residue is present in all PutAs and monofunctional GSALDHs. Hydrolysis of the acyl-enzyme intermediate yields the glutamate product, which is released from the enzyme. Finally, NADH dissociates, allowing NAD^+ to bind for a new round of catalysis.

The kinetic mechanism of the GSALDH module has been investigated in detail for EcPutA [52]. Global analysis of steady-state and single-turnover data are consistent with an ordered ternary mechanism in which the chemical step is rate limiting (Fig. 5B). Note that the chemical step of the ordered ternary mechanism (Fig. 5B) includes steps 1–3 of the catalytic cycle (Fig. 5A), so the kinetic data do not specify whether it is nucleophilic attack at the aldehyde, hydride transfer to NAD^+, or hydrolysis of the acyl-enzyme that limits the overall rate. Product inhibition by glutamate was not observed with glutamate at concentrations up to 50 mM. Also, proline was found to inhibit the GSALDH reaction (K_I = 80 mM).

Substrate channeling in PutA

Introduction to substrate channeling

PutA is an atypical flavoenzyme in that it is bifunctional and exhibits substrate channeling. Here the term "bifunctional" refers to an enzyme that catalyzes two different reactions using two distinct, spatially separated active sites. Substrate channeling is a process by which a metabolite (or intermediate) is transferred from one enzyme active site to another without freely diffusing into the surrounding bulk solvent [53].

Although unusual, other substrate-channeling bifunctional flavoenzymes are known (Table 3). For example, the ammonia-channeling amidotransferase glutamate synthase (GltS) catalyzes the conversion of L-glutamine and 2-oxoglutarate into two molecules of L-glutamate [54]. Ammonia generated from the hydrolysis of glutamine to glutamate in the

amidotransferase domain is channeled 32 Å to the FMN-binding domain, where it is added to 2-oxoglutarate to generate 2-iminoglutarate, followed by flavin-dependent reduction of 2-iminoglutarate to glutamate. Another example is dimethylglycine oxidase (DMGO), a bifunctional enzyme that has flavin oxidase and methylene transferase active sites separated by 40 Å [55]. The metabolic logic of channeling in DMGO is likely the protection of the unstable iminium intermediate [56]. Also, prokaryotes have bifunctional FAD biosynthetic enzymes that use flavins as substrates in sequential riboflavin kinase and FAD synthetase reactions [57, 58].

Potential physiological advantages of channeling include control of metabolic flux, protection of reactive and/or toxic intermediates, increased catalytic efficiency, and decreased diffusion of intermediates away from the catalytic sites [53]. Channeling may be particularly important for shuttling intermediates along a particular pathway in cases where substrates are present at concentrations lower than their cognate enzymes [53]. The primary advantages of substrate channeling in proline catabolism are thought to be protection of the reactive imine/aldehyde intermediate and the isolation of these intermediates from competing pathways of proline and arginine biosynthesis [27].

Why some bacteria have PutA rather than monofunctional PRODH and GSALDH is an open question. We note that the absence of PutA does not imply the absence of channeling. For example, the monofunctional PRODH and GSALDH enzymes from *Thermus thermophilus* have been shown to interact and channel the intermediate *in vitro* [59]. Thus, substrate channeling in proline catabolism may be widespread in life. If so, PutA may simply represent a refinement of a conserved metabolic strategy. Ultimately, answering such questions requires *in vivo* studies of substrate channeling. For example, it should be possible to study the effects of channeling *in vivo* with mutant forms of PutA that are defective in channeling but retain the individual catalytic activities. These studies are ongoing in our labs.

Channeling mechanisms include direct transfer through an internal tunnel, electrostatic channeling along the protein surface, and proximity effects [53, 60, 61]. The buried tunnel observed in all PutA structures clearly implies a direct substrate-channeling mechanism. The consistency of the protein fold and tunnel dimensions across four PutA classes (1A, 1B, 2A, 3B) implies a conserved substrate-channeling mechanism.

Steady-state kinetic evidence for substrate channeling in PutAs

Steady-state transient time analysis is commonly used to monitor channeling in PutA. Transient time analysis measures the progress curve of the time-dependent NADH formation in a coupled PRODH-GSALDH assay containing PutA, proline, an artificial electron acceptor (e.g. coenzyme Q_1), and NAD^+. The basis for this test is that the progress curve for uncoupled (non-channeling) PRODH and GSALDH enzymes can be simulated once the kinetic constants for the individual PRODH and GSALDH activities are known [52]. The coupled assay is then performed under conditions where the theoretical progress curve for the uncoupled enzymes has a substantial lag (typically a few minutes). Substrate channeling is indicated if the measured lag is substantially shorter than the predicted one for the uncoupled enzymes.

Trapping of the intermediate is also used to monitor substrate channeling in PutA. P5C is conveniently trapped with *o*-aminobenzaldehyde (*o*-AB) producing a dihydroquinazolinium compound. Like transient time analysis, trapping is done within the context of the coupled assay containing PutA, proline, an artificial electron acceptor, and NAD^+. The control experiment is an identical assay performed without NAD^+, which provides a measure of the maximum possible release of P5C into the bulk medium. The results are typically expressed as the percent of P5C trapped relative to the control.

Steady-state kinetics data are consistent with substrate channeling for all PutAs studied to date, including BjPutA [31], GsPutA [32], SmPutA [30], RcPutA [37], CfPutA [29], EcPutA [52], and a chimeric PutA consisting of the RHH domain of EcPutA fused to RcPutA [62]. Transient time analysis data collected on BjPutA are typical for PutAs (Fig. 6A). Whereas the predicted transient time for the uncoupled system is 9 min, the observed progress curve shows no discernible lag in the production of NADH. Similarly, P5C trapping is consistent with substrate channeling. BjPutA provides a representative example. Under the assay conditions, 70% of P5C generated in the PRODH site is channeled (Fig. 6B) [31]. A value of 50% was obtained for CfPutA [29].

A system for directly testing transient time known as “mixed variants transient time analysis” was developed for PutAs [63]. Instead of referencing the results to a theoretical progress curve for the uncoupled system, an experimental non-channeling control was generated using site-directed mutagenesis. Two PutA mutant variants are required. One is deficient in PRODH activity, and the other lacks GSALDH activity. An equimolar mixture of the two variants is the non-channeling control. The coupled assay of the mixed variants of BjPutA exhibits a lag time of 7 minutes (Fig. 6A). Mixed variant transient time analysis has also been performed with EcPutA [52].

Hysteresis in the PutA substrate-channeling step

The kinetic evidence for hysteresis in EcPutA

The complete kinetic mechanism has been worked out for EcPutA using global fitting of steady-state kinetic data, rapid reaction kinetic data, and ligand binding data [52]. The coupled PRODH-GSALDH activity of EcPutA is best described by a mechanism that includes a substrate channeling step linking the formation of P5C in the PRODH site to the binding of GSAL in the GSALDH site (Fig. 7A). Surprisingly, the microscopic rate constant for the PRODH-GSALDH coupled reaction from single turnover studies (0.037 s^{-1}) was 20 times lower than the corresponding steady-state k_{cat} (0.73 s^{-1}). This result contradicts the expectation that each forward obligatory first order step in the mechanism should have a rate constant higher than the steady-state k_{cat}. These results suggested the rate constant for the substrate channeling step increases with subsequent turnovers of the enzyme, implying that substrate channeling is an activated process, also known as hysteresis.

Hysteresis in EcPutA was explored by measuring the channeling rate constant as a function of the number of turnovers [52]. The channeling rate constant increases from 0.037 s^{-1} in the first turnover, to 0.40 s^{-1} after 5 turnovers and 0.90 s^{-1} after 25 turnovers. The number of turnovers required to achieve one-half of the steady-state rate constant is 15 turnovers (Fig.

7B). Equivalently, after 135 turnovers, the rate constant is 90% of the steady-state value. Simulation of the time-dependent activation of EcPutA channeling estimates the time required to activate half of the total enzyme population is $t_{1/2}$ = 22.9 s, which is very close to the time required to reach steady state of the NADH progress curve (transient time ~ 23.5 s) (Fig. 7C). This similarity of these two time scales suggests the observed lag in the steady-state progress curve is a reflection of the physical process that underlies the activation of substrate channeling. The current hypotheses about the physical basis for activation of channeling are discussed below.

The concept of enzyme hysteresis

Hysteresis refers to enzymes that respond slowly to a change in substrate concentration, resulting in a non-linear reaction progress curves [64]. This is possible, for example, when an isomerization process is rate-limiting. When conformational changes are slow relative to the measurement of the reaction rate, the change may lead to an enzyme form with different kinetic properties and cause a lag in the activation of the total enzyme population.

Thus, hysteretic behavior is a time-dependent effect that relates to the kinetic aspect of the chemical reaction and isolates the rate-limiting step in the conversion of one form of free enzyme or enzyme-substrate complex to a kinetically different form. The most convenient way to monitor a hysteretic behavior is to measure the time-dependent production of a product by continuous measurement of absorbance or fluorescence changes. This is commonly called a transient-time assay and the progress curve can be used to extrapolate from a linear phase and derive a lag time [64]. Enzyme hysteresis has been described in other complex mechanisms, including allosteric behavior arising from multiple substrate binding sites, and enzyme oligomerization. The physiological basis of hysteresis has been proposed to attenuate initial enzyme responses to metabolite fluctuations, thus allowing enzymes to reach maximum activity only under conditions of sustained metabolic changes [65]. A more detailed review about hysteretic enzymes can be found elsewhere [64].

Hypotheses about basis of enzyme hysteresis in PutA

EcPutA displays a slow hysteretic process for the overall coupled PRODH-GSALDH reaction reaching a steady-state k_{cat} of 0.73 s^{-1} after several turnovers [52]. Proline substrate binding is in rapid equilibrium with EcPutA and product release is not rate limiting for the overall reaction [52]. Also, there is no evidence of hysteresis in the individual PRODH and GSALDH catalytic reactions, therefore the underlying cause of hysteresis is likely associated with a substrate channeling step and the cavity connecting the active sites. We proposed two possible mechanisms for the observed hysteresis in EcPutA [52]. One mechanism is that the filling of the cavity with the intermediate P5C/GSAL prepares a fully activated channeling state of the enzyme and enhances transport of the intermediate between the active sites. This mechanism may involve expelling some of the water molecules that occupy the tunnel of the resting enzyme, and thus “flushing” the tunnel may contribute to hysteresis. The other mechanism involves optimization of the cavity leading to increased P5C hydrolysis and channeling activity.

The molecular basis of remodeling the cavity for enhanced substrate channeling is unclear, but crystal structures of the EcPutA PRODH domain [63, 66] and full-length GsPutA [32] show that the conformations of the flavin and the flavoenzyme active site are sensitive to the redox state of the flavin and the occupancy of the proline binding site. Reduction induces butterfly bending of the isoalloxazine ring and conformational change of the ribityl chain of the FAD. Further, substantial conformational changes associated with proline binding have been inferred from the crystal structure of GsPutA complexed with the proline analog THFA. The resting PRODH active site with oxidized FAD is open, and the binding of proline induces formation of a conserved ion pair and shifting of helix α8 (Fig. 8). These changes close the PRODH site and seal it from the substrate–channeling tunnel. The ion pair breaks again after the FAD is reduced and P5C is formed, permitting P5C to enter the tunnel. Another possibility is that conformational changes outside of the PRODH active site seal ancillary tunnels, reducing leakage of the intermediate. This possibility has been suggested for GsPutA as Asp321 rotates to block an ancillary exit tunnel in response to reduction of the FAD [32].

Hysteresis in other substrate channeling enzymes

Substrate channeling occurs in many other enzymes [56, 57, 67–69], but whether the channeling step is hysteretic remains to be determined. Interestingly, a few channeling systems show possible indicators of hysteretic channeling (Table 4). For example, a multienzyme synthase involved in a five-step synthesis of aromatic amino acids in the shikimate pathway exhibits a minute-long transient time persisting in the overall reaction [70]. When compared to a non-channeling system, the observation of the reduced transient time motivates a hypothesis that the change of the substrate concentration activates the multienzyme activity. Other examples of potentially hysteretic bifunctional enzymes that have been studied theoretically and experimentally are enzymes dihydrofolate reductase-thymidylate synthase and citrate synthase-malate dehydrogenase fusion protein [71]. Also, a trifunctional protein synthesizing 5,6-dihydroorotate has shown a transient time for the third reaction, however, it is not known whether the hysteretic behavior originates from substrate channeling [72].

PutA is a flavin switch protein

The flavin redox state has been shown to mediate protein interactions with other effector proteins, membranes, and nucleic acids, thereby regulating diverse biological processes such as metabolism, biosynthesis and cell survival. Proteins in which the flavin redox state controls the functional output of a protein are known as “flavin switch” proteins [28]. Flavin switch proteins respond to redox changes via hydrogen-binding and electrostatic interactions that link the flavin active site to the surface of the protein or nearby domains [28].

The mechanistic details of flavin switch proteins that respond to light sensing, changes in cellular redox conditions and intracellular substrate concentrations have been reviewed extensively [28]. Examples of flavin switch proteins that are well characterized include the light-oxygen-voltage (LOV) domain protein family and NifL from nitrogen fixing bacteria [28]. Another example is the flavoenzyme quinone reductase (NQO) which catalyzes the

two-electron reduction of ubiquinone and stabilizes the p53 tumor suppressor against proteasomal degradation in humans [73]. The modulation of the proteasome has also been shown in a yeast homolog quinone reductase Lot6p, which binds to the 20S proteasome and forms a ternary complex with transcriptional factor Yap4p [74, 75]. When binding to a specific inhibitor, the reduction of FAD leads to global changes in the NQO2 structure and stabilization of the active site in an alternate conformation [76], and the conformational switch is consistent with the observation of NQO1 in the redox-dependent regulation of p53 [77].

The enzymatic and transcriptional regulatory functions of trifunctional PutAs (type C) such as EcPutA are determined by the flavin redox state and its subcellular localization (Fig. 9). When the flavin cofactor is oxidized, EcPutA is cytosolic and functions as a transcriptional repressor of the *put* regulon via the N-terminal RHH domain. Reduction of the flavin by proline causes EcPutA to associate with the cytoplasmic membrane thereby enabling EcPutA to catalyze the proline:ubiquinone oxidoreductase reaction. The functional switching of PutA between transcriptional repressor and membrane-bound enzyme functions is dependent on intracellular proline levels, the redox state of the flavin cofactor, and conformational changes associated with reduction of the flavin [48].

The transcriptional repressor role of PutA

In *S. typhimurium* and *E. coli*, PutA is a primary regulator of the *put* regulon, which comprises the *putA* and *putP* genes that encode for the flavoenzyme PutA and the Na^+-proline transporter PutP, respectively [78, 79] (Fig. 9). PutA acts as an autogenous transcriptional repressor of the *put* regulon in the absence of proline by binding to the promoter region between the *putA* and *putP* genes [41]. When high concentrations of proline are available, PutA is released from the *put* regulon by proline reduction of the FAD cofactor and becomes strongly associated with the inner bacterial membrane, which contains quinone electron acceptors allowing PutA to complete the PRODH catalytic cycle [45].

The enzymatic and transport functions of the *put* genes are conserved among Gram-negative bacteria, but the genetic organization and regulatory mechanisms vary [80, 81]. In Gram-negative bacteria in which the *putA* and *putP* genes are transcribed divergently from the same intergenic region, trifunctional PutA acts a transcriptional repressor [41]. Gel-shift assays using different fragments of the *E. coli put* control DNA identified a consensus GTTGCA PutA binding site, which is found in other Gram-negative bacteria that share the same genetic arrangement of the *putA/P* genes as that of *E. coli* [41]. In *E. coli*, five binding sites are in the *putA/P* intergenic region. In addition to regulation by PutA, the *putA/P* genes are also subject to general catabolite and nitrogen regulation with high glucose repressing transcription of the *putA/P* genes [41].

Previous crystallographic research showed the DNA binding domain of *E. coli* PutA [40] consists of a dimeric assembly of two ribbon-helix-helix (RHH) folds – a β-strand followed by two helices that upon dimerization forms an intermolecular β-sheet. In the structure of the *E. coli* RHH-DNA complex, the intermolecular β-sheet inserts into the major groove of the DNA with a conserved triad of β-strand residues Thr5, Gly7 and Lys9 interacting with DNA bases [41]. The RHH-DNA binding footprint was found to extend beyond the

GTTGCA sequence to a 9-bp GGTTGCACC sequence [41]. Lys9 was shown to hydrogen bond to the palindromic GG/CC cap for optimal binding affinity [41]. Sequence variability in the region flanking the consensus GTTGCA binding site (i.e., lack of a GG/CC cap) is proposed to attenuate binding of PutA to the different sites in the *put* control DNA region of *E. coli* [41]. Consistent with this, the binding affinity of *E. coli* RHH to an oligomer with the GGTTGCACC sequence was shown to be 15-fold higher than to an oligomer that lacks the GG/CC cap (AGTTGCAAC) [41]. Other important binding interactions include RHH residues Thr28, Pro29, and His30 to the DNA backbone [41]. The overall binding of the RHH domain is entropy-driven indicating that desolvation of the PutA-DNA complex is important for DNA binding [41].

PutA is an unusual flavoenzyme as we are not aware of other flavoenzymes that also function as a DNA-binding transcriptional repressor. An example of another enzyme with transcriptional repressor activity, however, is RbkR, which controls riboflavin biosynthesis and metabolism in archaea. RbkR catalyzes the phosphorylation of riboflavin and very recently has been biochemically and structurally characterized [67]. The major difference between RbkR and PutA is that RbkR is not a flavoenzyme but uses riboflavin as a substrate, therefore it is a novel flavin metabolite-sensing transcriptional repressor. The RbkR regulon consists of the *rbkR* gene, riboflavin biosynthesis genes and vitamin uptake transporters. The autorepression of RbkR is stimulated by the substrate CTP and is repressed by FMN, the product of riboflavin kinase. The crystal structure reveals that RbkR is arranged as a homodimer in association with DNA through a N-terminal helix-turn-helix DNA binding domain, followed by a riboflavin kinase domain.

What is known about how PutA associates with membranes?

Bifunctional PutAs must interact with the membrane to couple electron transfer from proline to quinone electron acceptors in the membrane, thus completing the proline:ubiquinone oxidoreductase catalytic cycle. Structures of PutA in complex with a quinone analog and detergent molecules have provided insights into the quinone binding site and potential membrane interactions of PutAs [32]. Singh and coworkers captured an inactivated reduced form of GsPutA bound to the quinone analog, menadione bisulfite (MB). They used an approach of generating a stable form of the reduced enzyme using the mechanism-based inhibitor, *N*-propargylglycine (NPPG), to obtain a 1.95 Å resolution structure of reduced PutA with MB [32]. The structure revealed MB bound at the *si* face of the flavin isoalloxazine consistent with direct electron transfer from reduced flavin to quinone.

Clues into how PutA associates with the membrane were provided from a structure of GsPutA bound by a detergent molecule (Zwittergent 3–12, *N*-dodecyl-*N,N*-dimethyl-3-ammonio-1-propanesulfonate) [32]. The hydrocarbon tail of the detergent molecule binds to a hydrophobic patch in the α-domain of GsPutA, indicating that the α-domain has a role in PutA-membrane associations [32, 48]. This possibility is consistent with earlier proteolysis and fluorescence quenching experiments which identified a large conformational change in the α-domain upon proline reduction of the flavin [48, 82]. Thus far, redox dependent changes in the α-domain have not been observed by X-ray crystallography, however, this region is highly disordered in oxidized and reduced forms of PutAs suggesting significant

conformational flexibility [43, 66]. If the α-domain is critical for PutA-membrane binding, then according to a dimeric SAXS model of EcPutA, membrane- and DNA-binding likely involve the same interface. This model would be consistent with Maloy's hypothesis that membrane and DNA-binding are mutually exclusive [83] and that PutA-membrane binding is essential for not only catalytic activity but also cloaking the DNA-binding domain [42].

Evidence for the C-terminal ALDHSF domain of PutA being important for membrane binding has also been reported. Deletion of the C-terminal 26 residues of EcPutA generated a super-repressor PutA mutant that was devoid of membrane binding, suggesting the C-terminus contains critical membrane binding residues [84]. Further studies are needed to understand how the α-domain and C-terminal ALDHSF domains of PutA coordinate functional membrane binding.

The functional switching mechanism of PutA

The mechanism whereby PutA switches from a DNA-binding protein to a membrane-bound flavoenzyme is mediated by a proline-induced conformational change that is hypothesized to initiate at the flavin and traverse through the surrounding protein [85]. A proline-dependent conformational change is supported in part by limited proteolysis data that show praline reduction of the flavin induces a global conformational change involving the α-domain of EcPutA [48]. The three-dimensional structure of a full-length type C PutA is not yet known but molecular details for how flavin redox signals are transmitted out of the PRODH active site have emerged from other structures. Structures of a dithionite-reduced crystal of the *E. coli* PRODH domain and the *E. coli* PRODH domain inactivated with NPPG, which generates a covalently stable reduced state, have revealed significant conformational differences between the oxidized and reduced forms of the flavin cofactor (Fig. 10) [34, 43, 63, 66]. For example, the oxidized FAD is planar, whereas the reduced FAD cofactor adopts a highly nonplanar conformation with a butterfly bending angle of 22° around the N(5)-N(10) axis of the isoalloxazine ring [66]. Reduction of the FAD also induces a crankshaft rotation of the ribityl chain, which alters the hydrogen bonding interactions of the ribityl hydroxyl groups (Fig. 10). Furthermore, reduction of the flavin disrupts an interaction network linking the FAD N(5), Arg431, and Asp370 [63, 66]. A consequence of this disruption is that Asp370 rotates away from Arg431 and towards Glu372 on the β3-α3 loop of the PRODH domain [63] (Fig. 10).

The importance of some of these interactions in functional switching has been substantiated with biochemical studies. For example, site-directed mutagenesis implicated the linkage between the FAD N(5) and Glu372 as being critical for functional switching of EcPutA [66, 85]. Mutation of Arg431 or substitution of normal FAD with 5-deazaFAD, which lacks N(5), blocks EcPutA membrane binding [66]. Substitution of Asp370 or Glu372 with Ala also prevents EcPutA switching from a transcriptional repressor to a membrane-bound enzyme [85]. Although proline reduces the mutants Asp370Ala and Glu372Ala similarly to that of wild-type EcPutA, the mutants are unable to bind the membrane.

The above changes in the flavin active site have been shown to be necessary for redox-dependent PutA-membrane binding and accordingly must be transmitted out of the flavin active site to uncloak the EcPutA membrane domain(s) [48, 66, 82, 85]. Kinetic studies

using tryptophan fluorescence showed that the proline-dependent conformational change is much slower than FAD reduction [82], and is therefore not thought to be part of the catalytic cycle but rather is an isomerization step in the regulatory mechanism that directs PutA to the membrane [46]. Once the protein is membrane-bound, the conformational change is no longer necessary during subsequent turnovers allowing EcPutA to efficiently couple oxidation of proline to reduction of ubiquinone in the membrane (Fig. 9) [46]. As mentioned above, the C-terminal 26 residues of EcPutA are essential for membrane binding [84]. Surprisingly, RcPutA, a bifunctional class 1B PutA, also displays some aspects of switching, such as proline-induced membrane binding [62]. Thus, the C-terminal ALDHSF domain of RcPutA is not only essential for coupling PRODH/GSALDH activities and facilitating substrate channeling, but also enables RcPutA to toggle between soluble and membrane bound forms [37, 62]. The physiological importance of this for type B PutAs is not apparent, but it seems possible that some essential elements of functional switching are "hard-wired" in the PRODH and C-terminal ALDHSF domains of type B and C PutAs. Accordingly, in type A PutAs, which lack the C-terminal ALDHSF domain, membrane-binding is independent of proline [86].

Summary and concluding remarks

PutAs are bacterial bifunctional enzymes that combine PRODH and GSALDH activities into a single polypeptide chain. Some PutAs additionally function as transcriptional repressors of the *put* operon. These trifunctional PutAs are flavin switch proteins that change subcellular location and function in response to flavin reduction, allowing bacteria to adapt to the concentration of proline in the environment.

The PutA family exhibits an interesting diversity in oligomeric state and quaternary structure. The various shapes of PutA are different evolutionary solutions to the problem of sequestering a reactive metabolite (P5C/GSA). PutA oligomeric structure is correlated with domain architecture and function. Domain architecture type A PutAs function as domain-swapped dimers in which the oligomerization flap of one protomer enables substrate channeling in the other protomer. Type B PutAs form a different kind of dimer in which the C-terminal ALDHSF domain enables substrate channeling via tertiary structural interactions that mimic the quaternary structural interactions of type A PutAs. Additionally, type B PutAs are the only PutAs that can function as monomers. Type C PutAs dimerize via their DNA-binding domain, which reflects their transcriptional repressor function. In summary, oligomeric structure is intimately related to function in PutAs.

The consistency of the protein fold and tunnel dimensions in PutAs implies a conserved substrate-channeling mechanism. Furthermore, the observation of substrate channeling in PutA implies that in organisms where PRODH and GSALDH are encoded by different genes, the monofunctional enzymes interact and channel the intermediate. This hypothesis has been validated for the monofunctional enzymes form *Thermus thermophilus* [59]. Because human proline catabolic enzymes play multiple roles in health and disease, studying of the interaction between human PRODH and GSALDH is a major uncharted area of research.

PutA is an example of a hysteretic enzyme, whereby the substrate channeling step becomes activated with subsequent turnovers of the enzyme. This area of PutA biochemistry is relatively unstudied, so many outstanding questions about this phenomenon remain. For example, the underlying structural basis for hysteresis is unknown. The prevailing hypothesis is that activation involves conformational changes that seal leaky parts of tunnel system. Another issue is whether hysteresis also occurs in types A and B PutAs. Finally, the biological advantages of hysteresis remain to be determined.

Class 1C PutAs are remarkable trifunctional flavin switch proteins that change subcellular localization and function in response to environmental proline levels. Outstanding challenges in this area include determining the membrane-association surface of PutA and characterizing the redox-linked conformational changes that drive membrane association. Also, 1C PutA is the only class of PutA for which a crystal structure is lacking. Solving its structure would be a significant step forward in understanding the basis for activation of substrate channeling and redox-dependent functional switching.

Acknowledgments

Research reported in this publication was supported by the NIGMS of the National Institutes of Health under award numbers R01GM065546, R01GM061068, and P30GM103335.

Abbreviations used

ALDH	aldehyde dehydrogenase
ALDHSF	aldehyde dehydrogenase superfamily
BbPutA	*Bdellovibrio bacteriovorus* proline utilization A
BjPutA	*Bradyrhizobium japonicum* proline utilization A
CfPutA	*Corynebacterium freiburgense* proline utilization A
CS	chorismate synthase
DMGO	dimethylglycine oxidase
DrPRODH	*Deinococcus radiodurans* PRODH
EcPutA	*Escherichia coli* proline utilization A
GABA	γ-aminobutyric acid
GSAL	L-glutamate-γ-semialdehyde
GSALDH	L-glutamate-γ-semialdehyde dehydrogenase
GsPutA	*Geobacter sulfurreducens* proline utilization A
MB	menadione bisulfite
NQO	quinone reductase

***o*-AB**	*o*-aminobenzaldehyde
P5C	Δ^1-pyrroline-5-carboxylate
NPPG	*N*-propargylglycine
PRODH	proline dehydrogenase
PutA	proline utilization A
PDB	Protein Data Bank
RHH	ribbon-helix-helix
RcPutA	*Rhodobacter capsulatus* proline utilization A
SmPutA	*Sinorhizobium meliloti* proline utilization A
THFA	L-tetrahydro-2-furoic acid

References

1. Clelland CL, Read LL, Baraldi AN, Bart CP, Pappas CA, Panek LJ, Nadrich RH, Clelland JD. Evidence for association of hyperprolinemia with schizophrenia and a measure of clinical outcome. Schizophr. Res. 2011; 131(1–3):139–45. [PubMed: 21645996]
2. Jaeken J, Goemans N, Fryns JP, Francois I, de Zegher F. Association of hyperprolinaemia type I and heparin cofactor II deficiency with CATCH 22 syndrome: evidence for a contiguous gene syndrome locating the proline oxidase gene. J Inherit Metab Dis. 1996; 19(3):275–7. [PubMed: 8803768]
3. Srivastava D, Singh RK, Moxley MA, Henzl MT, Becker DF, Tanner JJ. The three-dimensional structural basis of type II hyperprolinemia. J Mol Biol. 2012; 420(3):176–89. [PubMed: 22516612]
4. Geraghty MT, Vaughn D, Nicholson AJ, Lin WW, Jimenez-Sanchez G, Obie C, Flynn MP, Valle D, Hu CA. Mutations in the Delta1-pyrroline 5-carboxylate dehydrogenase gene cause type II hyperprolinemia. Hum. Mol. Genet. 1998; 7(9):1411–5. [PubMed: 9700195]
5. Raux G, Bumsel E, Hecketsweiler B, van Amelsvoort T, Zinkstok J, Manouvrier-Hanu S, Fantini C, Breviere GM, Di Rosa G, Pustorino G, Vogels A, Swillen A, Legallic S, Bou J, Opolczynski G, Drouin-Garraud V, Lemarchand M, Philip N, Gerard-Desplanches A, Carlier M, Philippe A, Nolen MC, Heron D, Sarda P, Lacombe D, Coizet C, Alembik Y, Layet V, Afenjar A, Hannequin D, Demily C, Petit M, Thibaut F, Frebourg T, Campion D. Involvement of hyperprolinemia in cognitive and psychiatric features of the 22q11 deletion syndrome. Hum Mol Genet. 2007; 16(1):83–91. [PubMed: 17135275]
6. Willis A, Bender HU, Steel G, Valle D. PRODH variants and risk for schizophrenia. Amino Acids. 2008; 35(4):673–9. [PubMed: 18528746]
7. Duarte M, Afonso J, Moreira A, Antunes D, Ferreira C, Correia H, Marques M, Sequeira S. Hyperprolinemia as a clue in the diagnosis of a patient with psychiatric manifestations. Brain Dev. 2017; 39(6):539–541. [PubMed: 28202261]
8. Crabtree GW, Park AJ, Gordon JA, Gogos JA. Cytosolic Accumulation of L-Proline Disrupts GABA-Ergic Transmission through GAD Blockade. Cell Rep. 2016; 17(2):570–582. [PubMed: 27705802]
9. Liu W, Le A, Hancock C, Lane AN, Dang CV, Fan TW, Phang JM. Reprogramming of proline and glutamine metabolism contributes to the proliferative and metabolic responses regulated by oncogenic transcription factor c-MYC. Proc Natl Acad Sci U S A. 2012; 109(23):8983–8. [PubMed: 22615405]
10. Liu W, Phang JM. Proline dehydrogenase (oxidase) in cancer. Biofactors. 2012; 38(6):398–406. [PubMed: 22886911]

11. Phang JM, Liu W, Hancock CN, Fischer JW. Proline metabolism and cancer: emerging links to glutamine and collagen. Curr Opin Clin Nutr Metab Care. 2015; 18(1):71–7. [PubMed: 25474014]
12. Elia I, Broekaert D, Christen S, Boon R, Radaelli E, Orth MF, Verfaillie C, Grunewald TGP, Fendt SM. Proline metabolism supports metastasis formation and could be inhibited to selectively target metastasizing cancer cells. Nat Commun. 2017; 8:15267. [PubMed: 28492237]
13. Wanduragala S, Sanyal N, Liang X, Becker DF. Purification and characterization of Put1p from Saccharomyces cerevisiae. Arch. Biochem. Biophys. 2010; 498(2):136–42. [PubMed: 20450881]
14. Natarajan SK, Zhu W, Liang X, Zhang L, Demers AJ, Zimmerman MC, Simpson MA, Becker DF. Proline dehydrogenase is essential for proline protection against hydrogen peroxide-induced cell death. Free radical biology & medicine. 2012; 53(5):1181–91. [PubMed: 22796327]
15. Liu W, Zabirnyk O, Wang H, Shiao YH, Nickerson ML, Khalil S, Anderson LM, Perantoni AO, Phang JM. miR-23b targets proline oxidase, a novel tumor suppressor protein in renal cancer. Oncogene. 2010; 29(35):4914–24. [PubMed: 20562915]
16. Donald SP, Sun XY, Hu CA, Yu J, Mei JM, Valle D, Phang JM. Proline oxidase, encoded by p53-induced gene-6, catalyzes the generation of proline-dependent reactive oxygen species. Cancer Res. 2001; 61(5):1810–5. [PubMed: 11280728]
17. Zarse K, Schmeisser S, Groth M, Priebe S, Beuster G, Kuhlow D, Guthke R, Platzer M, Kahn CR, Ristow M. Impaired insulin/IGF1 signaling extends life span by promoting mitochondrial L-proline catabolism to induce a transient ROS signal. Cell Metab. 2012; 15(4):451–65. [PubMed: 22482728]
18. Szabados L, Savoure A. Proline: a multifunctional amino acid. Trends Plant Sci. 2010; 15(2):89–97. [PubMed: 20036181]
19. Liang X, Zhang L, Natarajan SK, Becker DF. Proline Mechanisms of Stress Survival. Antioxid Redox Signal. 2013; 19(9):998–1011. [PubMed: 23581681]
20. Zhang L, Alfano JR, Becker DF. Proline metabolism increases katG expression and oxidative stress resistance in Escherichia coli. J Bacteriol. 2015; 197(3):431–40. [PubMed: 25384482]
21. Tanner JJ. Structural biology of proline catabolism. Amino Acids. 2008; 35(4):719–30. [PubMed: 18369526]
22. Nakajima K, Inatsu S, Mizote T, Nagata Y, Aoyama K, Fukuda Y, Nagata K. Possible involvement of put A gene in Helicobacter pylori colonization in the stomach and motility. Biomed. Res. 2008; 29(1):9–18. [PubMed: 18344593]
23. Krishnan N, Doster AR, Duhamel GE, Becker DF. Characterization of a Helicobacter hepaticus putA mutant strain in host colonization and oxidative stress. Infect. Immun. 2008; 76(7):3037–44. [PubMed: 18458068]
24. Cheng Z, Lin M, Rikihisa Y. Ehrlichia chaffeensis Proliferation Begins with NtrY/NtrX and PutA/GlnA Upregulation and CtrA Degradation Induced by Proline and Glutamine Uptake. mBio. 2014; 5(6):e02141–14. [PubMed: 25425236]
25. Nagata K, Nagata Y, Sato T, Fujino MA, Nakajima K, Tamura T. L-Serine, D- and L-proline and alanine as respiratory substrates of Helicobacter pylori: correlation between in vitro and in vivo amino acid levels. Microbiology. 2003; 149(Pt 8):2023–30. [PubMed: 12904542]
26. Singh RK, Tanner JJ. Unique structural features and sequence motifs of proline utilization A (PutA). Front Biosci (Landmark Ed). 2012; 17:556–68. [PubMed: 22201760]
27. Arentson BW, Sanyal N, Becker DF. Substrate channeling in proline metabolism. Front. Biosci. 2012; 17:375–88.
28. Becker DF, Zhu W, Moxley MA. Flavin redox switching of protein functions. Antioxid. Redox Signal. 2011; 14(6):1079–91. [PubMed: 21028987]
29. Korasick D, Gamage TT, Christgen S, Stiers KM, Beamer LJ, Henzl MT, Becker DF, Tanner JJ. Structure and characterization of a class 3B proline utilization A: ligand-induced dimerization and importance of the C-terminal domain for catalysis. J Biol Chem. 2017 In press.
30. Luo M, Gamage TT, Arentson BW, Schlasner KN, Becker DF, Tanner JJ. Structures of Proline Utilization A (PutA) Reveal the Fold and Functions of the Aldehyde Dehydrogenase Superfamily Domain of Unknown Function. J. Biol. Chem. 2016; 291(46):24065–24075. [PubMed: 27679491]
31. Srivastava D, Schuermann JP, White TA, Krishnan N, Sanyal N, Hura GL, Tan A, Henzl MT, Becker DF, Tanner JJ. Crystal structure of the bifunctional proline utilization A flavoenzyme from

Bradyrhizobium japonicum. Proc. Natl. Acad. Sci. USA. 2010; 107(7):2878–83. [PubMed: 20133651]

32. Singh H, Arentson BW, Becker DF, Tanner JJ. Structures of the PutA peripheral membrane flavoenzyme reveal a dynamic substrate-channeling tunnel and the quinone-binding site. Proc. Nat. Acad. Sci. USA. 2014; 111(9):3389–94. [PubMed: 24550478]
33. Korasick DA, Singh H, Pemberton TA, Luo M, Dhatwalia R, Tanner JJ. Biophysical investigation of type A PutAs reveals a conserved core oligomeric structure. FEBS J. 2017 Accepted.
34. Luo M, Arentson BW, Srivastava D, Becker DF, Tanner JJ. Crystal structures and kinetics of monofunctional proline dehydrogenase provide insight into substrate recognition and conformational changes associated with flavin reduction and product release. Biochemistry. 2012; 51(50):10099–108. [PubMed: 23151026]
35. Arentson BW, Luo M, Pemberton TA, Tanner JJ, Becker DF. Kinetic and Structural Characterization of Tunnel-Perturbing Mutants in Bradyrhizobium japonicum Proline Utilization A. Biochemistry. 2014; 53(31):5150–61. [PubMed: 25046425]
36. Krissinel E, Henrick K. Secondary-structure matching (SSM), a new tool for fast protein structure alignment in three dimensions. Acta Crystallogr. D Biol. Crystallogr. 2004; 60(Pt 12 Pt 1):2256–68. [PubMed: 15572779]
37. Luo M, Christgen S, Sanyal N, Arentson BW, Becker DF, Tanner JJ. Evidence That the C-Terminal Domain of a Type B PutA Protein Contributes to Aldehyde Dehydrogenase Activity and Substrate Channeling. Biochemistry. 2014; 53(35):5661–73. [PubMed: 25137435]
38. Jaffe EK. Morpheeins--a new structural paradigm for allosteric regulation. Trends Biochem. Sci. 2005; 30(9):490–7. [PubMed: 16023348]
39. Selwood T, Jaffe EK. Dynamic dissociating homo-oligomers and the control of protein function. Arch. Biochem. Biophys. 2012; 519(2):131–43. [PubMed: 22182754]
40. Larson JD, Jenkins JL, Schuermann JP, Zhou Y, Becker DF, Tanner JJ. Crystal structures of the DNA-binding domain of Escherichia coli proline utilization A flavoprotein and analysis of the role of Lys9 in DNA recognition. Protein Sci. 2006; 15:1–12. [PubMed: 16373473]
41. Zhou Y, Larson JD, Bottoms CA, Arturo EC, Henzl MT, Jenkins JL, Nix JC, Becker DF, Tanner JJ. Structural basis of the transcriptional regulation of the proline utilization regulon by multifunctional PutA. J. Mol. Biol. 2008; 381(1):174–88. [PubMed: 18586269]
42. Singh RK, Larson JD, Zhu W, Rambo RP, Hura GL, Becker DF, Tanner JJ. Small-angle X-ray Scattering Studies of the Oligomeric State and Quaternary Structure of the Trifunctional Proline Utilization A (PutA) Flavoprotein from Escherichia coli. J. Biol. Chem. 2011; 286(50):43144–53. [PubMed: 22013066]
43. Lee YH, Nadaraia S, Gu D, Becker DF, Tanner JJ. Structure of the proline dehydrogenase domain of the multifunctional PutA flavoprotein. Nat. Struct. Biol. 2003; 10(2):109–114. [PubMed: 12514740]
44. Arnold K, Bordoli L, Kopp J, Schwede T. The SWISS-MODEL workspace: a web-based environment for protein structure homology modelling. Bioinformatics. 2006; 22(2):195–201. [PubMed: 16301204]
45. Moxley MA, Tanner JJ, Becker DF. Steady-state kinetic mechanism of the proline:ubiquinone oxidoreductase activity of proline utilization A (PutA) from Escherichia coli. Arch. Biochem. Biophys. 2011; 516(2):113–20. [PubMed: 22040654]
46. Moxley MA, Becker DF. Rapid reaction kinetics of proline dehydrogenase in the multifunctional praline utilization A protein. Biochemistry. 2012; 51(1):511–20. [PubMed: 22148640]
47. Menzel R, Roth J. Enzymatic properties of the purified putA protein from Salmonella typhimurium. J. Biol. Chem. 1981; 256(18):9762–6. [PubMed: 6270101]
48. Zhu W, Becker DF. Flavin redox state triggers conformational changes in the PutA protein from Escherichia coli. Biochemistry. 2003; 42(18):5469–77. [PubMed: 12731889]
49. Pemberton TA, Tanner JJ. Structural basis of substrate selectivity of Delta(1)-pyrroline-5-carboxylate dehydrogenase (ALDH4A1): Semialdehyde chain length. Arch. Biochem. Biophys. 2013; 538(1):34–40. [PubMed: 23928095]
50. Bottoms CA, Smith PE, Tanner JJ. A structurally conserved water molecule in Rossmann dinucleotide-binding domains. Protein Sci. 2002; 11(9):2125–37. [PubMed: 12192068]

51. Christensen EM, Patel SM, Korasick DA, Campbell AC, Krause KL, Becker DF, Tanner JJ. Resolving the Cofactor Binding Site in the Proline Biosynthetic Enzyme Human Pyrroline-5-Carboxylate Reductase 1. J. Biol. Chem. 2017 In press; published online March 3, 2017.
52. Moxley MA, Sanyal N, Krishnan N, Tanner JJ, Becker DF. Evidence for Hysteretic Substrate Channeling in the Proline Dehydrogenase and Delta1-Pyrroline-5-carboxylate Dehydrogenase Coupled Reaction of Proline Utilization A (PutA). J. Biol. Chem. 2014; 289(6):3639–51. [PubMed: 24352662]
53. Anderson KS. Fundamental mechanisms of substrate channeling. Methods Enzymol. 1999; 308:111. [PubMed: 10507003]
54. van den Heuvel RH, Curti B, Vanoni MA, Mattevi A. Glutamate synthase: a fascinating pathway from L-glutamine to L-glutamate. Cell Mol Life Sci. 2004; 61(6):669–81. [PubMed: 15052410]
55. Leys D, Basran J, Scrutton NS. Channelling and formation of 'active' formaldehyde in dimethylglycine oxidase. EMBO J. 2003; 22(16):4038–48. [PubMed: 12912903]
56. Tralau T, Lafite P, Levy C, Combe JP, Scrutton NS, Leys D. An internal reaction chamber in dimethylglycine oxidase provides efficient protection from exposure to toxic formaldehyde. J. Biol. Chem. 2009; 284(26):17826–17834. [PubMed: 19369258]
57. Herguedas B, Lans I, Sebastian M, Hermoso JA, Martinez-Julvez M, Medina M. Structural insights into the synthesis of FMN in prokaryotic organisms. Acta Crystallogr D Biol Crystallogr. 2015; 71(Pt 12):2526–42. [PubMed: 26627660]
58. Herguedas B, Martinez-Julvez M, Frago S, Medina M, Hermoso JA. Oligomeric state in the crystal structure of modular FAD synthetase provides insights into its sequential catalysis in prokaryotes. J Mol Biol. 2010; 400(2):218–30. [PubMed: 20471397]
59. Sanyal N, Arentson BW, Luo M, Tanner JJ, Becker DF. First evidence for substrate channeling between proline catabolic enzymes: a validation of domain fusion analysis for predicting protein-protein interactions. J. Biol. Chem. 2015; 290(4):2225–2234. [PubMed: 25492892]
60. Miles EW, Rhee SG, Davies DR. The molecular basis of substrate channeling. J. Biol. Chem. 1999; 274(18):12193–12196. [PubMed: 10212181]
61. Knighton DR, Kan CC, Howland E, Janson CA, Hostomska Z, Welsh KM, Matthews DA. Structure of and kinetic channelling in bifunctional dihydrofolate reductase-thymidylate synthase. Nat Struct Biol. 1994; 1(3):186–94. [PubMed: 7656037]
62. Arentson BW, Hayes EL, Zhu W, Singh H, Tanner JJ, Becker DF. Engineering a trifunctional praline utilization A chimaera by fusing a DNA-binding domain to a bifunctional PutA. Bioscience reports. 2016; 36(6):e00413. [PubMed: 27742866]
63. Srivastava D, Zhu W, Johnson WH Jr, Whitman CP, Becker DF, Tanner JJ. The structure of the praline utilization a proline dehydrogenase domain inactivated by N-propargylglycine provides insight into conformational changes induced by substrate binding and flavin reduction. Biochemistry. 2010; 49(3):560–569. [PubMed: 19994913]
64. Frieden C. Slow transitions and hysteretic behavior in enzymes. Annual review of Biochemistry. 1979; 48:471–89.
65. Wu Z, Xing J. Functional roles of slow enzyme conformational changes in network dynamics. Biophys. J. 2012; 103(5):1052–9. [PubMed: 23009855]
66. Zhang W, Zhang M, Zhu W, Zhou Y, Wanduragala S, Rewinkel D, Tanner JJ, Becker DF. Redox-induced changes in flavin structure and roles of flavin N(5) and the ribityl 2'-OH group in regulating PutA-membrane binding. Biochemistry. 2007; 46(2):483–91. [PubMed: 17209558]
67. Rodionova IA, Vetting MW, Li X, Almo SC, Osterman AL, Rodionov DA. A novel bifunctional transcriptional regulator of riboflavin metabolism in Archaea. Nucleic acids research. 2017; 45(7): 3785–3799. [PubMed: 28073944]
68. van den Heuvel RHH, Ferrari D, Bossi RT, Ravasio S, Curti B, Vanoni MA, Florencio FJ, Mattevi A. Structural studies on the synchronization of catalytic centers in glutamate synthase. J. Biol. Chem. 2002; 277(27):24579–24583. [PubMed: 11967268]
69. Dunn MF, Aguilar V, Brzović P, Drewe WF, Houben KF, Leja CA, Roy M. The tryptophan synthase bienzyme complex transfers indole between the alpha- and beta-sites via a 25–30 A long tunnel. Biochemistry. 1990; 29(37):8598–8607. [PubMed: 2271543]

70. Welch GR, Gaertner FH. Influence of an aggregated multienzyme system on transient time: kinetic evidence for compartmentation by an aromatic-amino-acid synthesizing complex of Neurospora crassa. Proc Natl Acad Sci U S A. 1975; 72(11):4218–22. [PubMed: 128001]

71. Elcock AH, Huber GA, McCammon JA. Electrostatic channeling of substrates between enzyme active sites: comparison of simulation and experiment. Biochemistry. 1997; 36(51):16049–16058. [PubMed: 9405038]

72. Christopherson RI, Jones ME. The overall synthesis of L-5 6-dihydroorotate by multienzymatic protein pyr1–3 from hamster cells. Kinetic studies, substrate channeling, and the effects of inhibitors. J Biol Chem. 1980; 255(23):11381–95. [PubMed: 6108323]

73. Sollner S, Macheroux P. New roles of flavoproteins in molecular cell biology: an unexpected role for quinine reductases as regulators of proteasomal degradation. FEBS J. 2009; 276(16):4313–24. [PubMed: 19624732]

74. Liger D, Graille M, Zhou CZ, Leulliot N, Quevillon-Cheruel S, Blondeau K, Janin J, van Tilbeurgh H. Crystal structure and functional characterization of yeast YLR011wp, an enzyme with NAD(P)H-FMN and ferric iron reductase activities. J Biol Chem. 2004; 279(33):34890–7. [PubMed: 15184374]

75. Sollner S, Deller S, Macheroux P, Palfey BA. Mechanism of Flavin Reduction and Oxidation in the Redox-Sensing Quinone Reductase Lot6p from Saccharomyces cerevisiae. Biochemistry. 2009; 48(36):8636–8643. [PubMed: 19618916]

76. Leung KK, Shilton BH. Chloroquine binding reveals flavin redox switch function of quinone reductase 2. J Biol Chem. 2013; 288(16):11242–51. [PubMed: 23471972]

77. Asher G, Lotem J, Cohen B, Sachs L, Shaul Y. Regulation of p53 stability and p53-dependent apoptosis by NADH quinone oxidoreductase 1. Proc Natl Acad Sci U S A. 2001; 98(3):1188–93. [PubMed: 11158615]

78. Hahn DR, Myers RS, Kent CR, Maloy SR. Regulation of proline utilization in Salmonella typhimurium: molecular characterization of the put operon, and DNA sequence of the put control region. Molecular & general genetics : MGG. 1988; 213(1):125–133. [PubMed: 2851701]

79. Nakao T, Yamato I, Anraku Y. Mapping of the multiple regulatory sites for putP and putA expression in the putC region of Escherichia coli. Molecular & general genetics : MGG. 1988; 214(3):379–388. [PubMed: 2464125]

80. Chen LM, Maloy S. Regulation of proline utilization in enteric bacteria: cloning and characterization of the Klebsiella put control region. J Bacteriol. 1991; 173(2):783–90. [PubMed: 1987164]

81. Jafri S, Evoy S, Cho K, Craighead HG, Winans SC. An Lrp-type transcriptional regulator from Agrobacterium tumefaciens condenses more than 100 nucleotides of DNA into globular nucleoprotein complexes. J Mol Biol. 1999; 288(5):811–24. [PubMed: 10329181]

82. Zhu W, Becker DF. Exploring the proline-dependent conformational change in the multifunctional PutA flavoprotein by tryptophan fluorescence spectroscopy. Biochemistry. 2005; 44(37):12297–306. [PubMed: 16156643]

83. Muro-Pastor AM, Ostrovsky P, Maloy S. Regulation of Gene Expression by Repressor Localization: Biochemical Evidence that Membrane and DNA Binding by the PutA Protein are Mutually Exclusive. J. Bacteriol. 1997; 179(8):2788–2791. [PubMed: 9098084]

84. Zhou Y, Zhu W, Bellur PS, Rewinkel D, Becker DF. Direct linking of metabolism and gene expression in the proline utilization A protein from Escherichia coli. Amino Acids. 2008; 35(4): 711–8. [PubMed: 18324349]

85. Zhu W, Haile AM, Singh RK, Larson JD, Smithen D, Chan JY, Tanner JJ, Becker DF. Involvement of the beta3-alpha3 loop of the proline dehydrogenase domain in allosteric regulation of membrane association of proline utilization A. Biochemistry. 2013; 52(26):4482–91. [PubMed: 23713611]

86. Zhang W, Krishnan N, Becker DF. Kinetic and thermodynamic analysis of Bradyrhizobium japonicum PutA-membrane associations. Archives of biochemistry and biophysics. 2006; 445(1): 174–183. [PubMed: 16310755]

87. Menzel R, Roth J. Purification of the putA gene product. A bifunctional membrane-bound protein from Salmonella typhimurium responsible for the two-step oxidation of proline to glutamate. J. Biol. Chem. 1981; 256(18):9755–9761. [PubMed: 6270100]

88. Kitzing K, Macheroux P, Amrhein N. Spectroscopic and kinetic characterization of the bifunctional chorismate synthase from Neurospora crassa: evidence for a common binding site for 5-enolpyruvylshikimate 3-phosphate and NADPH. J Biol Chem. 2001; 276(46):42658–66. [PubMed: 11526120]

89. Quevillon-Cheruel S, Leulliot N, Meyer P, Graille M, Bremang M, Blondeau K, Sorel I, Poupon A, Janin J, van Tilbeurgh H. Crystal structure of the bifunctional chorismate synthase from Saccharomyces cerevisiae. J. Biol. Chem. 2004; 279(1):619–625. [PubMed: 14573601]

90. Binda C, Bossi RT, Wakatsuki S, Arzt S, Coda A, Curti B, Vanoni MA, Mattevi A. Cross-Talk and Ammonia Channeling between Active Centers in the Unexpected Domain Arrangement of Glutamate Synthase, Structure (London, England : 1993). 2000; 8(12):1299–1308.

91. Sievers F, Wilm A, Dineen D, Gibson TJ, Karplus K, Li W, Lopez R, McWilliam H, Remmert M, Soding J, Thompson JD, Higgins DG. Fast, scalable generation of high-quality protein multiple sequence alignments using Clustal Omega. Molecular systems biology. 2011; 7:539. [PubMed: 21988835]

92. Dereeper A, Guignon V, Blanc G, Audic S, Buffet S, Chevenet F, Dufayard JF, Guindon S, Lefort V, Lescot M, Claverie JM, Gascuel O. Phylogeny.fr: robust phylogenetic analysis for the non-specialist. Nucleic Acids Res. 2008; 36:W465–9. Web Server issue. [PubMed: 18424797]

93. Luo M, Gates KS, Henzl MT, Tanner JJ. Diethylaminobenzaldehyde is a covalent, irreversible inactivator of ALDH7A1. ACS Chem Biol. 2015; 10(3):693–7. [PubMed: 25554827]

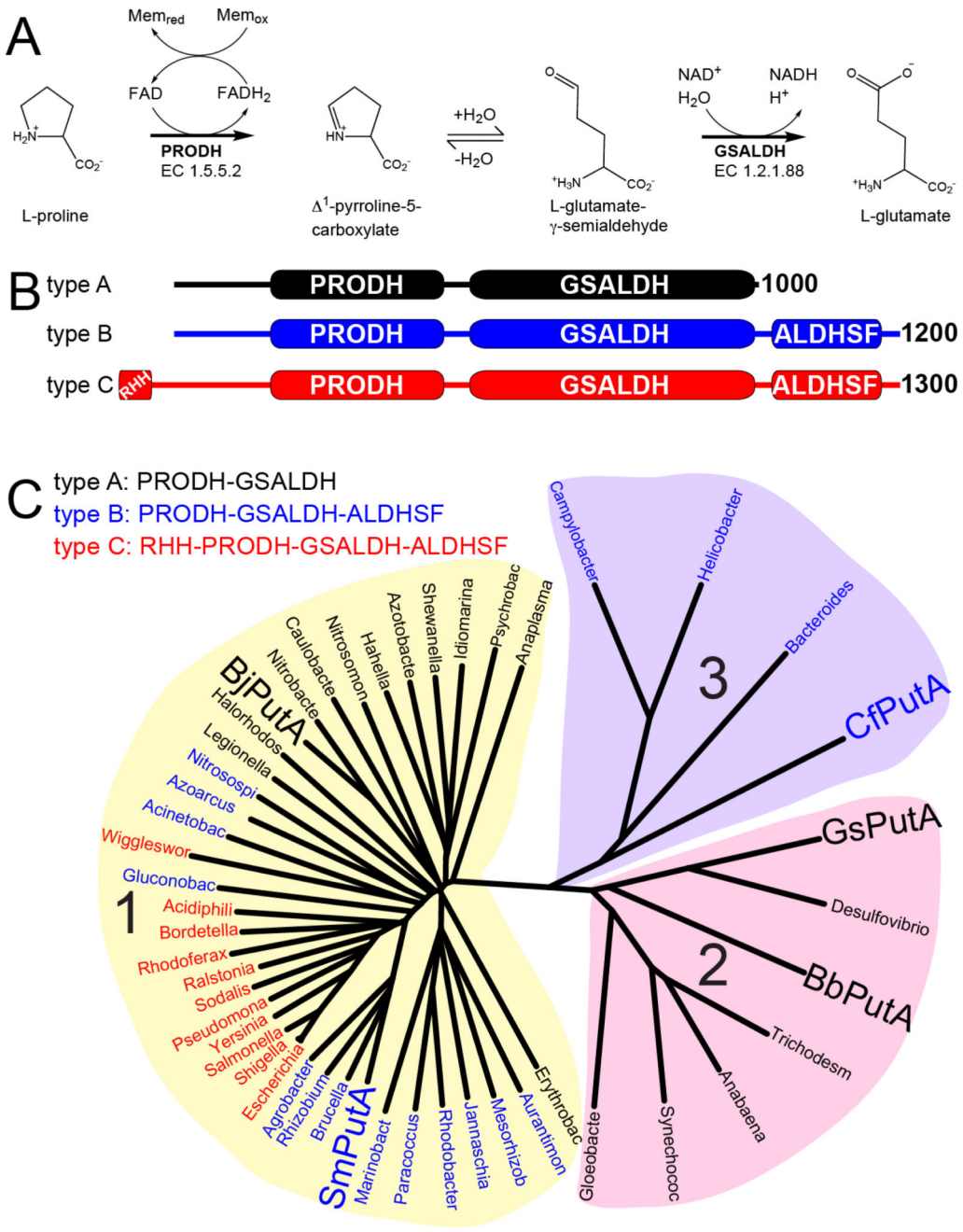

Fig. 1.

The reactions of proline catabolism and classification of PutAs. (A) The reactions catalyzed by the PRODH and GSALDH domains of PutA. (B) The three domain architectures of PutAs. (C) Phylogenetic tree based on a global sequence alignment of PutAs. Architecture types A, B, and C are indicated by black, blue, and red font, respectively. The PutAs for which crystal structures have been determined are noted in large font. The alignment was calculated with Clustal Omega [91] and visualized with DrawTree [92]. This figure was adapted from Korasick, et al. [29].

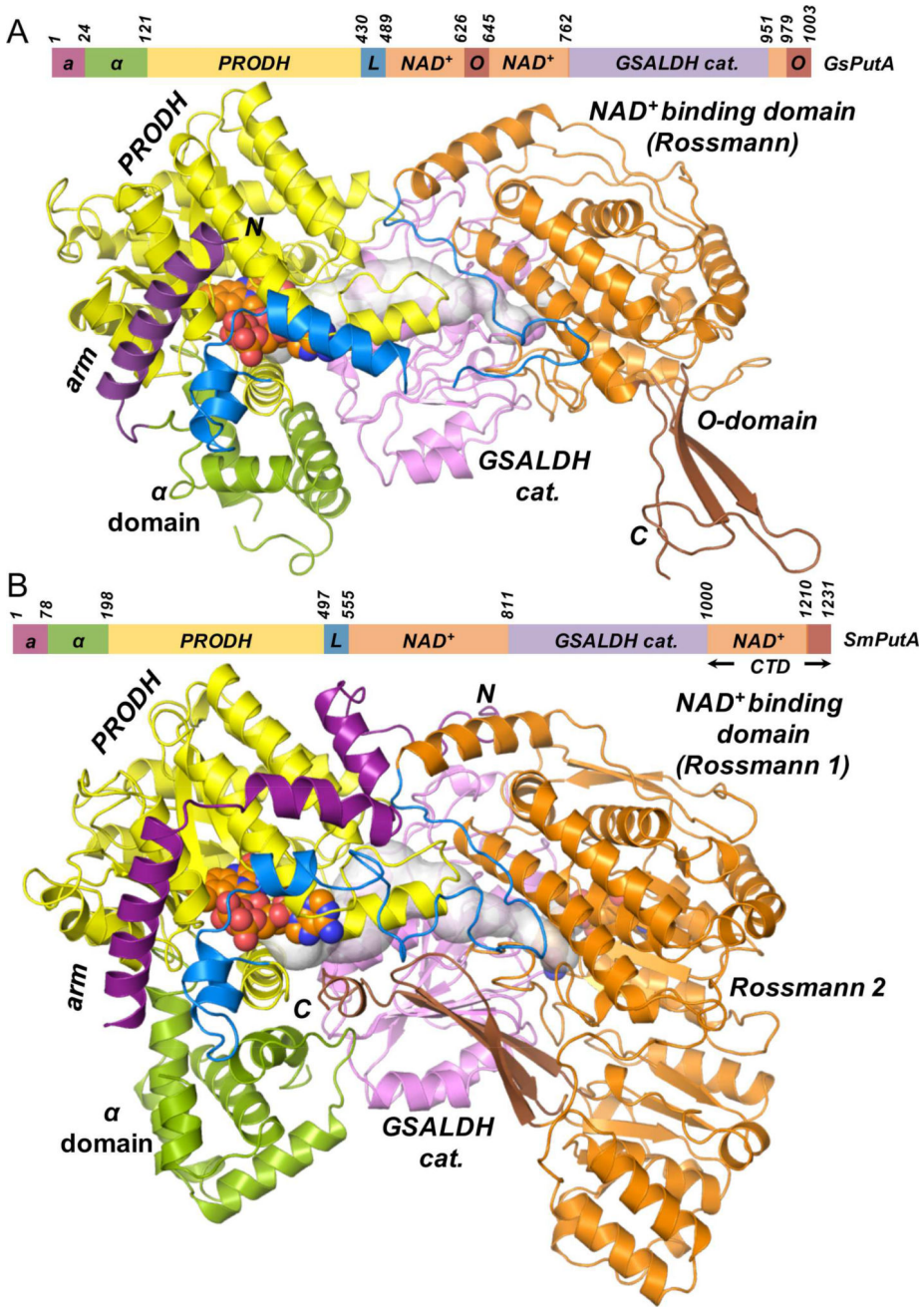

Fig. 2.

Crystal structures of type A and B PutAs. (A) The class 2A GsPutA (PDB 4NM9). (B) The class 1B PutA SmPutA (PDB 5KF6). The grey surface represents the substrate-channeling tunnel. FAD is drawn as orange spheres.

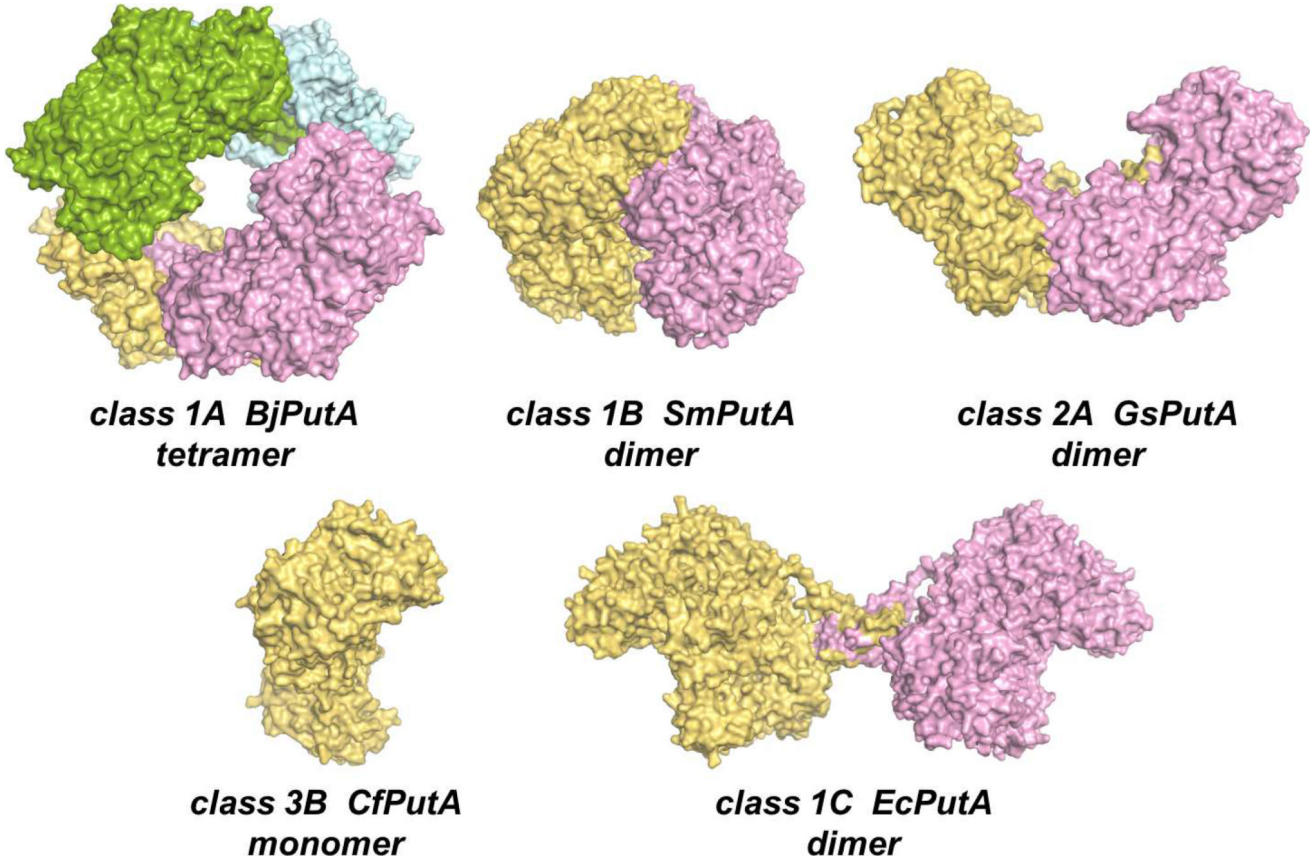

Fig. 3.

Comparison of oligomeric structures of five PutAs in surface representation, including BjPutA (PDB 3HAZ), SmPutA (PDB 5KF6), GsPutA (PDB 4NM9), CfPutA (PDB 5UX5), and EcPutA (a SAXS rigid body model). The scale applies to all the structures.

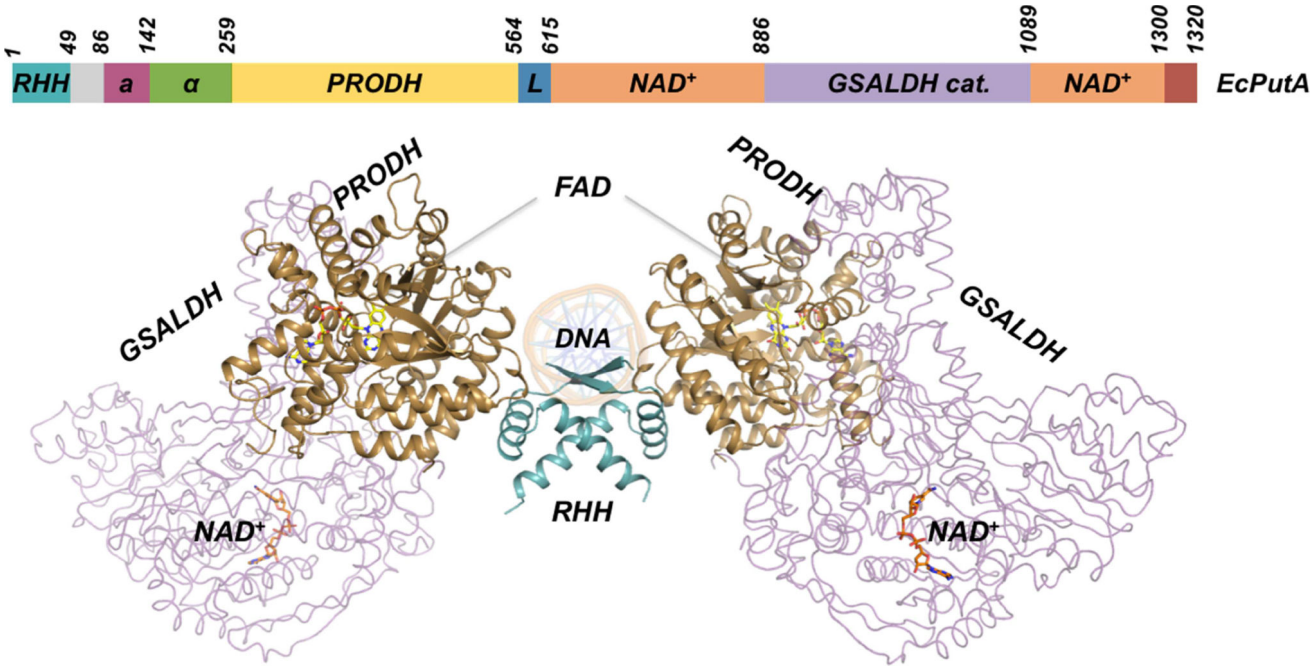

Fig. 4.

Domain diagram of the class 1C EcPutA and a SAXS rigid body model of EcPutA in complex with DNA.

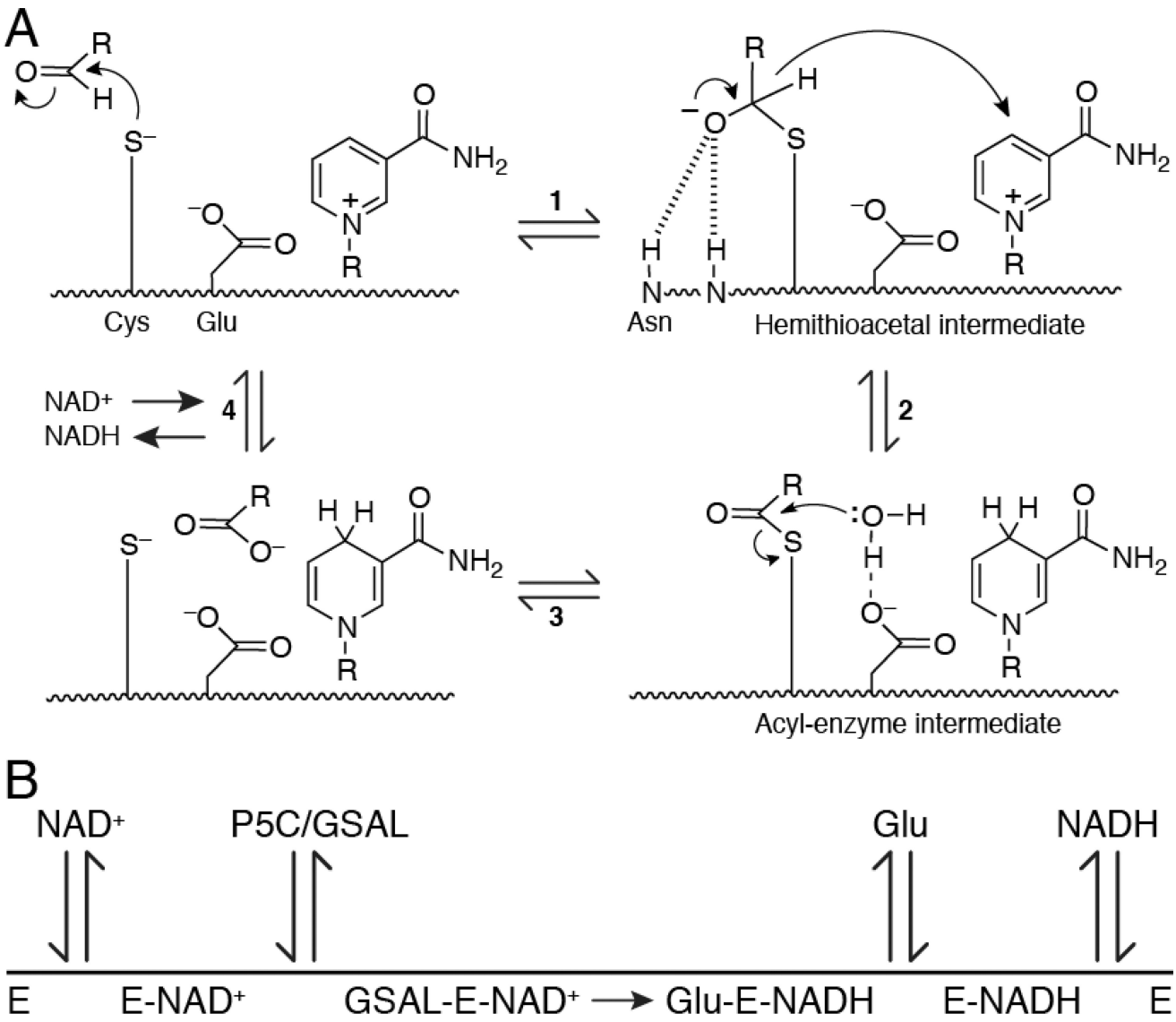

Fig. 5.

The catalytic mechanism of GSALDH. (A) The major steps in the catalytic cycle of ALDHSF enzymes. (1) Nucleophilic attack by the catalytic cysteine on the aldehyde produces a hemithioacetal intermediate. Hydrogen bond donors in the oxyanion hole stabilize the negative charge of the hemithioacetal intermediate. (2) Hydride transfer to NAD^+ generates NADH and the acyl-enzyme intermediate. (3) A conserved glutamate residue activates the water molecule that attacks the acyl-enzyme intermediate. Hydrolysis of the acyl-enzyme intermediate yields the product glutamate, which is released from the enzyme. (4) NADH dissociates and NAD^+ binds to regenerate the active enzyme. (B) The ordered ternary mechanism of the GSALDH module of EcPutA determined from steady-state and single-turnover experiments [52]. This figure was adapted from Luo et al. [93] and Moxley et al. [52].

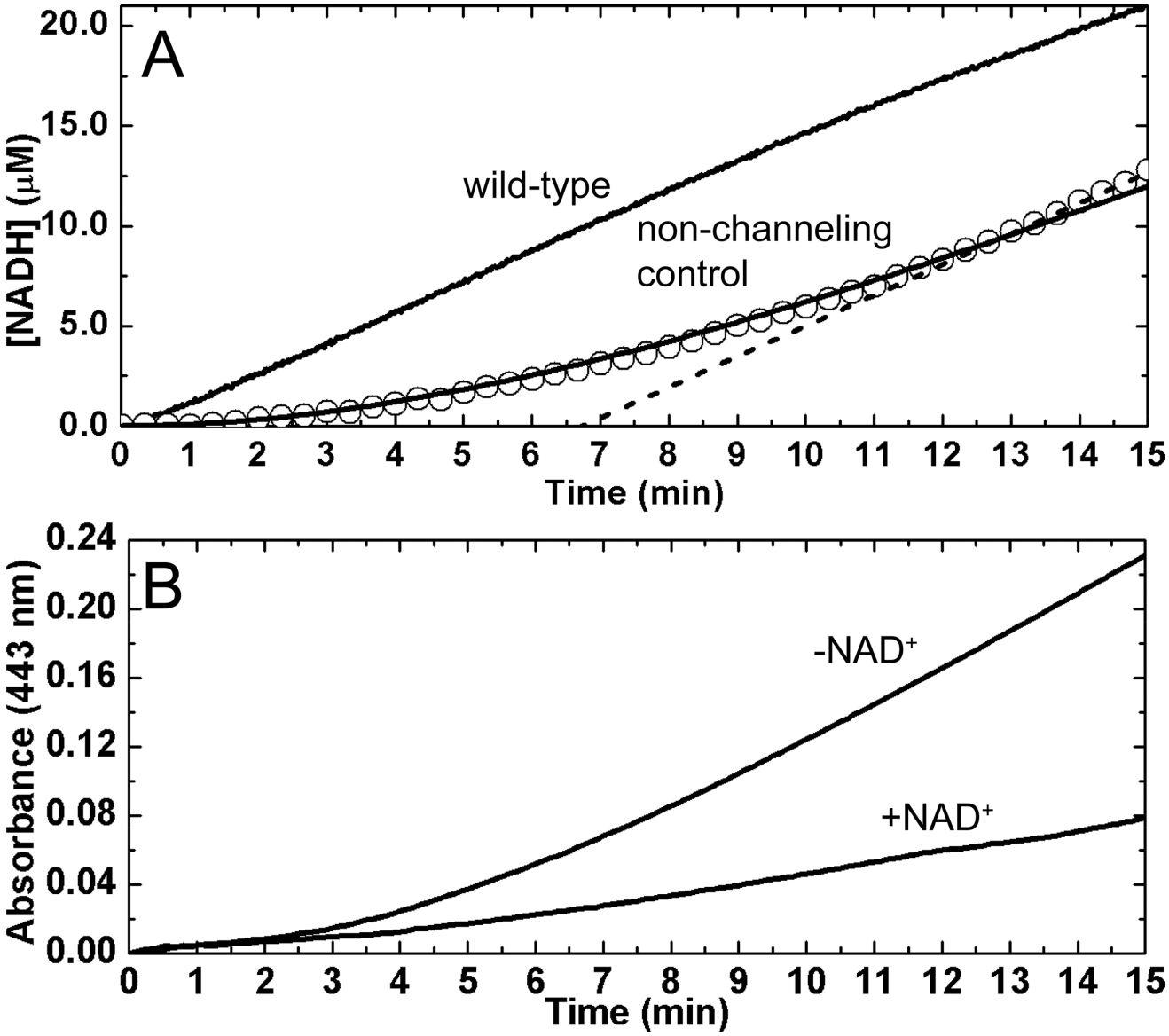

Fig. 6.

Kinetic evidence for substrate channeling in BjPutA. (A) NADH formation by wild-type BjPutA (upper solid curve) and a non-channeling control consisting of an equimolar mixture of monofunctional variants R456M and C792A (circles). The solid curve overlaying the data for the non-channeling control was calculated from a theoretical model for uncoupled PRODH and P5CDH and extrapolates to a transient time of 9 minutes. The dashed line represents the extrapolation used to estimate the transient time for the mixed variants non-channeling control (transient time of 7 minutes). (B) P5C trapping experiments performed in the presence and absence of NAD^+. This figure was adapted from [31].

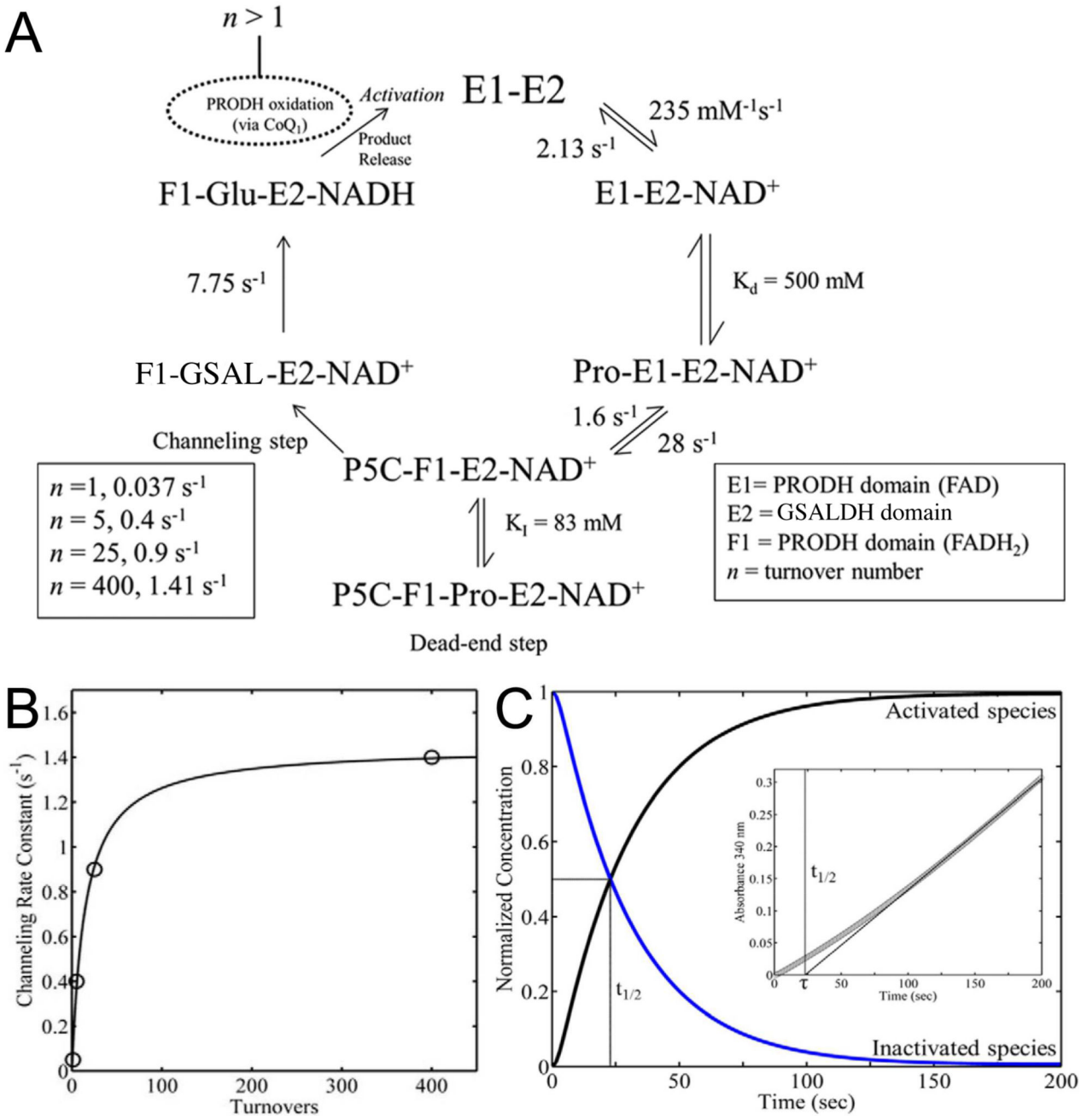

Fig. 7.

Hysteretic substrate channeling mechanism of EcPutA. (A) The channeling model used for fitting PRODH-GSALDH coupled activity in EcPutA with best fit rate constants and equilibrium constants shown for each step. (B) Dependence of the channeling rate constant on the number of enzyme turnovers. (C) Simulation of the time-dependent activation of the channeling step in EcPutA. The concentrations of the activated and non-activated enzyme species are shown as black and blue curves, respectively. Inset: EcPutA PRODH-GSALDH coupled progress curve data with the same substrate concentrations used for the simulation in the main figure. The linear portion of the progress curve was fitted to a line and is

extrapolated to estimate the transient time (23.5 s) to reach steady state. This figure was adapted from Moxley et al. [52].

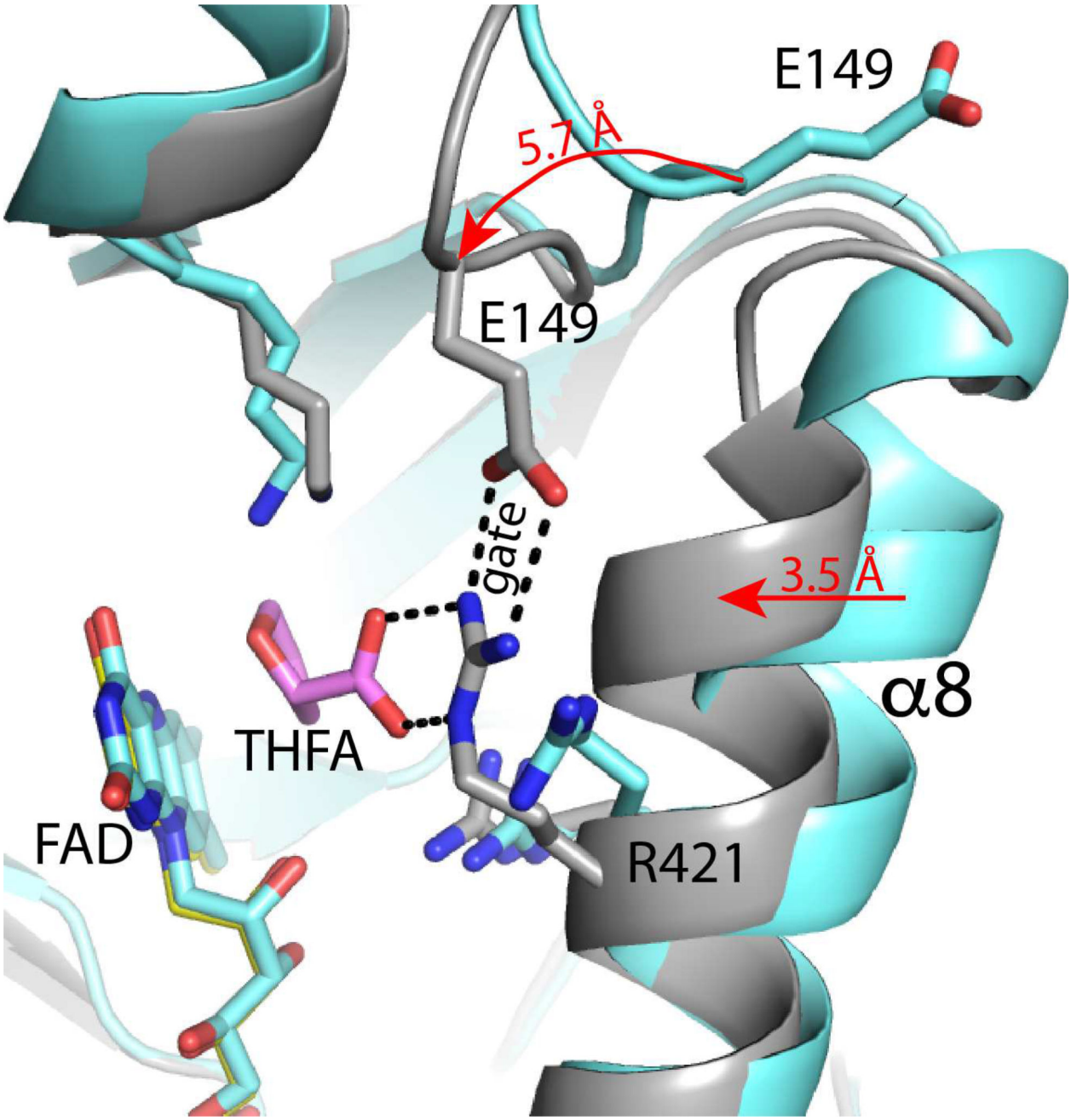

Fig. 8. Conformational changes within the PRODH site induced by proline binding

Comparison of the open (cyan) and THFA-bound closed (gray) PRODH active sites in GsPutA (PDB codes 4NM9 and 4NMA). The arrows show the directions of conformational changes that accompany THFA binding. Figure adapted from [32].

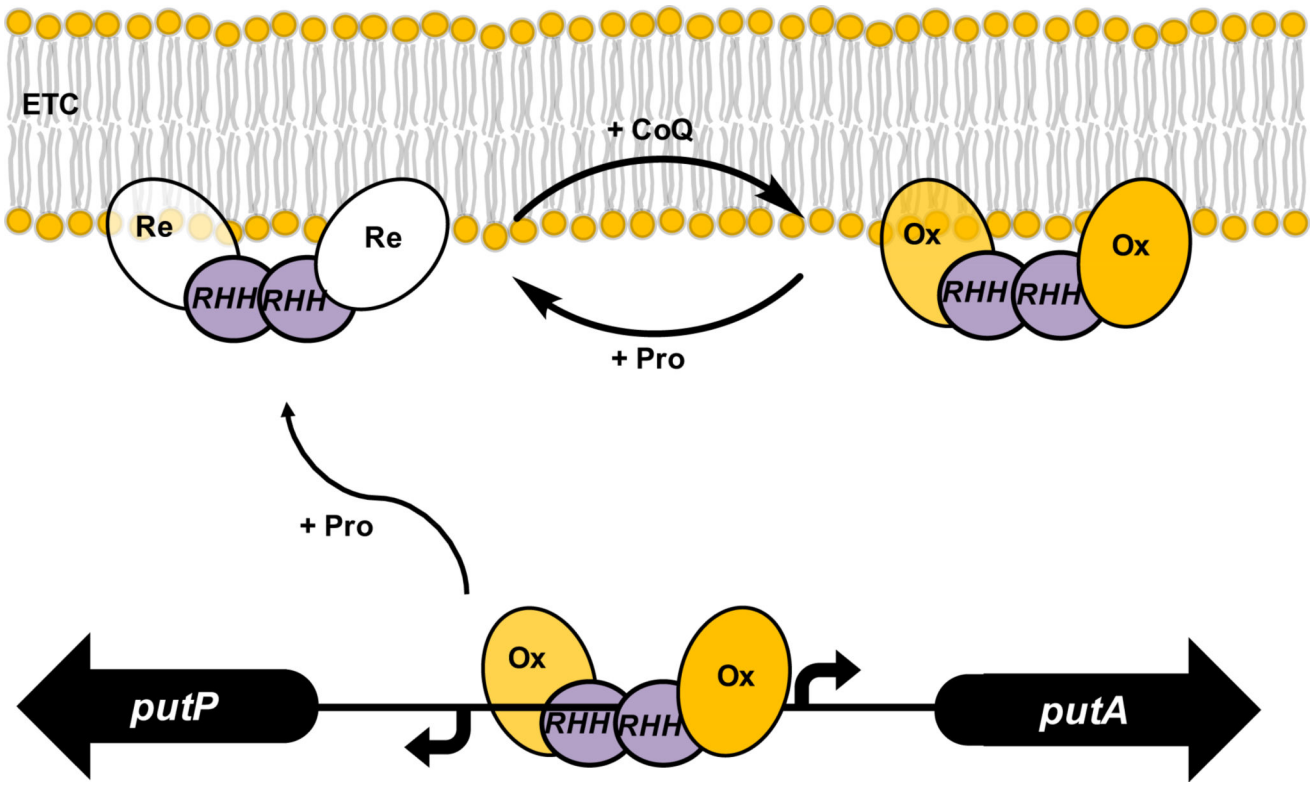

Fig. 9.

Model of PutA functional switching. In the absence of proline, PutA represses expression the *put* operon by binding to operator sites located between the genes for PutA and the proline transporter PutP. In the presence of an activating concentration of proline, PutA associates with the inner membrane, where it couples proline oxidation with the reduction of ubiquinone in the electron transport chain.

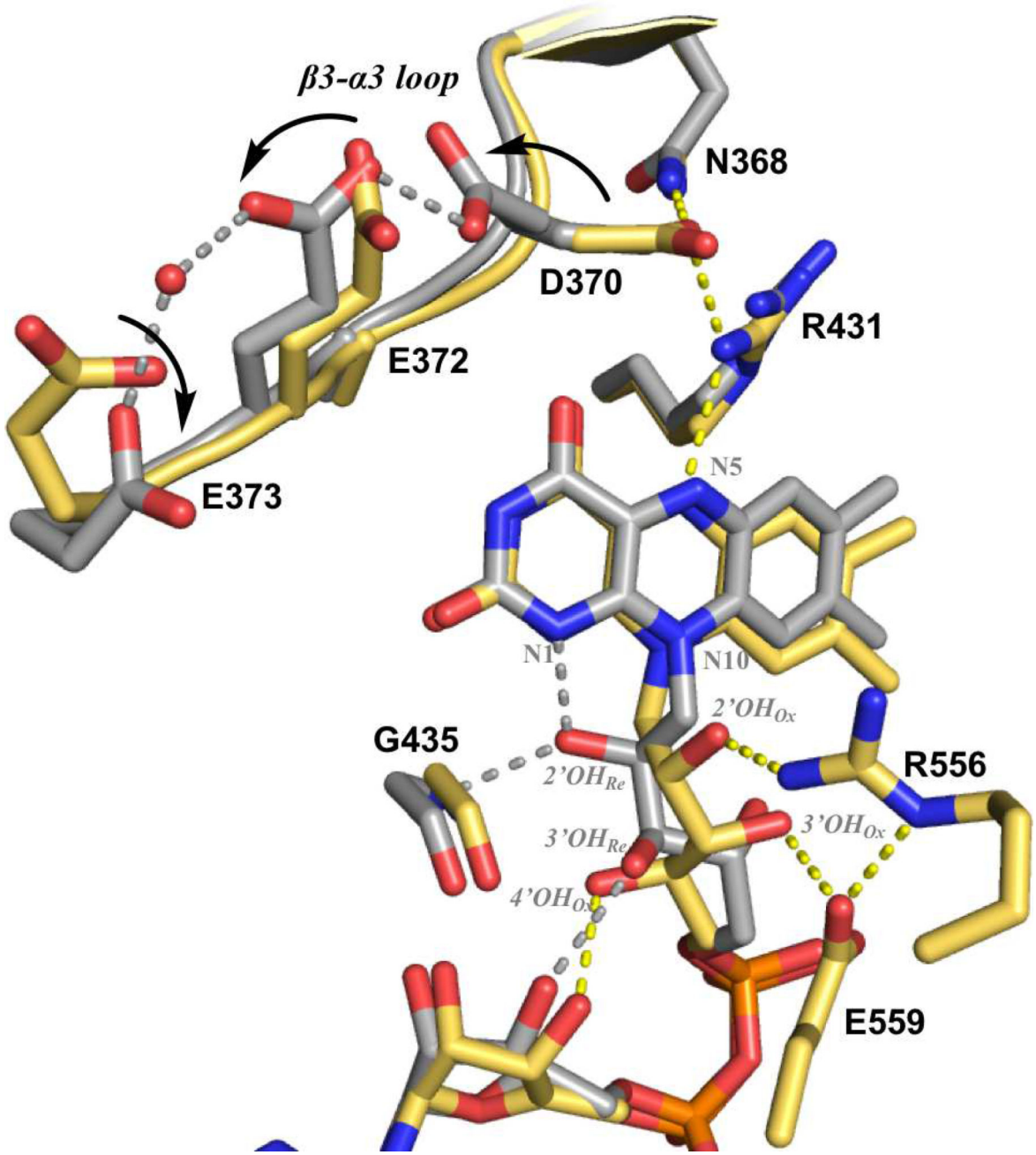

Fig. 10.

Structural overlay of the β3-α3 loop regions of the oxidized EcPutA PRODH domain complexed with THFA (yellow, PDB 1TIW) and the EcPutA PRODH domain inactivated by NPPG (gray, PDB 3ITG). Yellow and gray dashed lines represent electrostatic interactions in oxidized THFA complex and NPPG-inactivated enzyme, respectively. The arrows denote conformational changes induced by enzyme inactivation (i.e. reduction).

Table 1

Oligomeric states and quaternary structures of PutA

Enzyme	PutA class	Oligomeric state	Quaternary structure	R_g (Å)[a]	Reference
BjPutA	1A	Tetramer	Ring formed of two classic ALDHSF domain-swapped dimers	51	[31]
GsPutA	2A	Dimer	Classic ALDHSF domain-swapped dimer	44	[32]
BbPutA	2A	Dimer	Classic ALDHSF domain-swapped dimer	45	[33]
SmPutA	1B	Monomer/dimer	Packing of the C-terminal ALDHSF domain against α-helices of the catalytic modules	33/40	[30]
CfPutA	3B	Monomer/dimer	Unknown	32/−	[29]
EcPutA	1C	Dimer	Intermolecular β-sheet from the RHH domain	63	[42]

[a]Radius of gyration from the crystal structure or SAXS.

Table 2

Crystal structures of PutA

Enzyme	PutA class	PDB code	Resolution (Å)	FAD redox state	PRODH ligands	GSALDH ligands	Reference
BjPutA	1A	3HAZ	2.1	Oxidized	FAD/Sulfate	NAD^+	[31]
BjPutA D779W	1A	4Q71	2.2	Oxidized	FAD		[35]
BjPutA D779Y	1A	4Q72	2.3	Oxidized	FAD		[35]
BjPutA D778Y	1A	4Q73	2.3	Oxidized	FAD		[35]
GsPutA	2A	4NM9	1.9	Oxidized	FAD		[32]
GsPutA	2A	4NMA	2.1	Oxidized	FAD/L-THFA		[32]
GsPutA	2A	4NMB	2.2	Oxidized	FAD/L-lactate	MES	[32]
GsPutA	2A	4NMC	1.9	Oxidized	FAD/L-lactate/Zwittergent		[32]
GsPutA	2A	4NMD	1.98	Reduced	FAD		[32]
GsPutA	2A	4NME	2.09	Reduced	FAD/NPPG		[32]
GsPutA	2A	4NMF	1.95	Reduced	FAD/NPPG/Menadione		[32]
BbPutA	2A	5UR2	2.23	Reduced	FAD/NPPG		[33]
SmPutA	1B	5KF6	1.7	Oxidized	FAD/L-THFA	NAD^+	[30]
SmPutA	1B	5KF7	1.9	Oxidized	FAD/L-THFA	NAD^+	[30]
CfPutA	3B	5UX5	2.7	Oxidized	FAD	NAD^+	[29]

Table 3

Bifunctional flavoenzymes

Enzyme	Functions	Cofactor	Reference
PutA	Proline dehydrogenase and glutamate semialdehyde dehydrogenase	FAD	[87]
Chorismate synthase from fungus	Chorismate synthase and flavin reductase	FMN	[88, 89]
Dimethylglycine oxidase from bacteria	Oxidase and methylene transferase	FAD	[55, 56]
Glutamate synthase from bacteria	Amidotransferase and glutamate synthase	FMN	[68, 90]

Table 4

Other enzymes that possibly exhibit hysteresis in substrate channeling

Enzyme	Function	Reference
A multienzyme complex of *Neurospora crassa*	Five-step synthesis of aromatic amino acids	[70]
Dihydrofolate reductase-thymidylate synthase	Supply 2-deoxythymidylate for DNA synthesis	[60, 71]
Citrate synthase-malate dehydrogenase fusion protein	Channel oxaloacetate in the Krebs tricarboxylic acid cycle	[71]
ME *pyr*1–3	A trifunctional protein in the biosynthesis of pyrimidine in mammals	[72]